Plasma Metabolomic and Lipidomic Alterations Associated with COVID-19

Di Wu[1,2,9], Ting Shu[3,4,2,9], Xiaobo Yang[5,9], Jian-Xin Song[6,9], Mingliang Zhang[7,9], Wen Liu[3,4], Muhan Huang[1,2], Yuan Yu[5], Qingyu Yang[3,4,2], Tingju Zhu[3,4], Jiqian Xu[5], Jingfang Mu[1,2], Yaxin Wang[5], Hong Wang[7], Tang Tang[7], Yujie Ren[1,2], Yongran Wu[5], Yang Qiu[1,2,3,8]*, Ding-Yu Zhang[3,4]*, You Shang[5,3,4]*, Xi Zhou[1,2,3,8,10]*

[1] Joint Laboratory of Infectious Diseases and Health, Wuhan Institute of Virology & Wuhan Jinyintan Hospital, Wuhan Institute of Virology, Center for Biosafety Mega-Science, Chinese Academy of Sciences (CAS), Wuhan, Hubei 430023 China

[2] State Key Laboratory of Virology, Wuhan Institute of Virology, Center for Biosafety Mega-Science, CAS, Wuhan, Hubei 430071, China

[3] Center for Translational Medicine, Jinyintan Hospital, Wuhan, Hubei 430023 China

[4] Joint Laboratory of Infectious Diseases and Health, Wuhan Institute of Virology & Wuhan Jinyintan Hospital, Wuhan Jinyintan Hospital, Wuhan, Hubei 430023 China

[5] Department of Critical Care Medicine, Union Hospital, Tongji Medical College, Huazhong University of Science and Technology, Wuhan, Hubei 430030 China

[6] Department of Infectious Diseases, Tongji Hospital, Tongji Medical College, Huazhong University of Science and Technology, Wuhan, Hubei 430030 China

[7] Wuhan Metware Biotechnology Co., Ltd, Wuhan, Hubei 430075 China

[8] University of Chinese Academy of Sciences, Beijing 100049 China

[9] These authors contributed equally

[10] Lead Contact

*Correspondence: yangqiu@wh.iov.cn (Y.Q.), zhangdy@hotmail.com (D.-Y.Z.), you_shanghust@163.com (Y.S.), zhouxi@wh.iov.cn (X.Z.)

Abstract

The pandemic of the coronavirus disease 2019 (COVID-19) has become a global public health crisis. COVID-19 is marked by its rapid progression from mild to severe conditions, particularly in the absence of adequate medical care. However, the physiological changes associated with COVID-19 are barely understood. In this study, we performed untargeted metabolomic and lipidomic analyses of plasma from a cohort of COVID-19 patients who had experienced different symptoms. We found the metabolite and lipid alterations exhibit apparent correlation with the course of disease in these COVID-19 patients, indicating that the development of COVID-19 affected patient metabolism. Moreover, many of the metabolite and lipid alterations, particularly ones associated with hepatic functions, have been found to align with the progress and severity of COVID-19. This work provides valuable knowledge about blood biomarkers associated with COVID-19 and potential therapeutic targets, and presents important resource for further studies of COVID-19 pathogenesis.

Introduction

The outbreak of COVID-19, which emerged from Wuhan, China since December 2019, has rapidly spread to almost every corners of the world and been declared a pandemic by the World Health Organization (WHO). Up to the date of March 31, 2020, there are over 750,000 confirmed COVID-19 cases and about 36,000 deaths worldwide according to the situation report of WHO. Based on a recent study of 44,672 confirmed COVID-19 cases up to February 11 by Chinese Center for Disease Control and Prevention, over 19% COVID-19 patients developed severe or critical conditions (1). The global fatality rate is around 4.8% in all the confirmed cases until March 31, and has even reached 10% in some developed countries probably due to a more elderly population (2).

The main attacking organ of COVID-19 is lung, and some patients develop life-threatening acute respiratory distress syndrome (ARDS). Besides, the attacks of liver, muscle, gastrointestinal tract, lymph node, and heart by COVID-19 have also been found or proposed (3-6). On the other hand, although more than 80% COVID-19 patients experienced only mild symptoms, it has been found that the conditions can rapidly progress from mild to severe ones, particularly in the absence of adequate medical care. Moreover, the mortality rate of COVID-19 in critically ill cases can be over 60%, posing great pressure on treatment (7). However, the physiological changes associated with COVID-19 under different symptomatic conditions are barely understood.

Metabolites and lipids are major molecular constituents in human plasma. During

critical illness, metabolic and lipid abnormalities are commonly observed, which are believed to contribute to physiology and pathology. Moreover, previous studies have demonstrated dramatic alterations of metabolome and lipidome in human plasma caused by various diseases including viral infections, such as Ebola virus disease (8, 9). Here, we performed the untargeted metabolomic and lipidomic profilings of plasma samples collected from a cohort of COVID-19 patients, including COVID-19 fatalities and survivors recovered from mild or severe symptoms. Our findings here show many of the metabolite and lipid alterations, particularly ones associated with hepatic functions, align with the progress and severity of the disease, which would provide valuable knowledge about blood biomarkers associated with COVID-19 as well as potential therapeutic targets, and shed light into the pathogenesis of COVID-19.

Results

Study design and patients

Blood samples were collected at Wuhan Jinyintan Hospital from COVID-19 patients with laboratory confirmed severe acute respiratory syndrome coronavirus 2 (SARS-CoV-2) infection. Serial samples were collected over the course of disease from 9 patients with fatal (F) outcome (F1-F4), 11 patients diagnosed as severe (S) symptoms (S1-S2), and 14 patients diagnosed as mild (M) symptoms (M1-M2) (Table S1). Of note, all the patients in the severe (S) and mild (M) groups had survived from COVID-19 and been discharged from hospital. F1 represents the first samples collected from the COVID-19 fatal patients, while F4 represents the last samples before additional samples could be collected. S1 or M1 represents the samples during the disease peak of the patients in the S or M group as being determined based on the Diagnosis and Treatment Protocol for Novel Coronavirus Pneumonia (6th edition) published by the National Health Commission of China (10), while S2 or M2 represents the last samples collected from patients in each group before their discharge from hospital. For comparison, the blood samples from 10 healthy volunteers were collected. Metabolites and lipids were extracted from the same plasma sample separated from the whole blood, and analyzed using liquid chromatography electrospray ionisation tandem mass spectrometry (LC-ESI-MS/MS) system. The orthogonal partial least-squares discriminant analysis (OPLS-DA) was used to discriminate metabolomics profiles between the groups of COVID-19 patients and healthy people (Figure S1-S4). In total, 431 metabolites and 698 lipids were identified and quantified, and both metabolome

and lipidome showed dramatic alterations in the plasma of these COVID-19 patients (Table S2 and S3).

Plasma metabolomic alternations correspond to clinical symptoms of COVID-19

For different courses of fatal COVID-19 patients (F1-F4), we analyzed the metabolites that underwent significant change [F4 vs. H, >1 $\log_2$ fold change (FC) <-1, typically P <0.05]. For F vs. H, 87 of the total 431 metabolites were significantly different (P < 0.05) at F1, while the number of significantly altered metabolites were increased to 162 at F4 in the fatalities; and most of the changes are down-regulation (Table S2). We found a positive correlation between the alteration of metabolites and the course of disease deterioration in fatal patients (Figure 1A and Table S4), indicating that the development of disease affects the metabolism of metabolites. A prominent signature observed among fatal COVID-19 patients was an acute reduction of free amino acids in patient plasma over the course of COVID-19. For instance, L-Malic acid exhibited the greatest $\log_2$ FC (-5.2) among all significantly altered amino acids in the fatalities. These free amino acids are rapidly consumed in inflammatory states to provide energy and materials for the proliferation and phagocytosis of immune cells (11), indicating that immune system were activated in these cases.

The changes in nucleotide and organic acid metabolisms of COVID-19 fatalities are complicated. We observed that the levels of some nucleotides and organic acids were significantly increased (e.g., hypoxanthine), whereas the levels of some nucleotides and organic acids were significantly reduced [e.g., Guanosine

Monophosphate (GMP)]. Hypoxanthine-guanine phosphoribosyl transferase (HPRT) is an important enzyme involved in nucleotide recycle pathway and can covert hypoxanthine and guanine to inosine 5'-monophosphate (IMP) and GMP, respectively (12, 13). The observed abnormal levels of hypoxanthine and GMP suggested that the function of HPRT had become defective in these COVID-19 fatal patients, which could result in the disorders of purine and pyrimidine metabolism. In addition, we observed that the level of carbamoyl phosphate was significantly and gradually reduced over the course of COVID-19 fatalities. Carbamoyl phosphate is synthesized from free amino donors by carbamoyl phosphate synthetase I (CPSI) in mitochondria of liver cells, and participates in the urea cycle to remove excess ammonia and produce urea (14-17). Its reduction in fatal cases of COVID-19 suggests the possibility of liver damage, which could also impair amino acid metabolism.

We also profiled the metabolites in the different courses of severe and mild COVID-19 patients (S1 and S2; M1 and M2), and analyzed those that underwent the significant change [S1 vs. H, >1 $\log_2$ FC <-1, typically P <0.05; M1 vs. H, >1 $\log_2$ FC <-1, typically P <0.05] (Figure 1B and Table S5). There are apparently less metabolites with significant changes (>1 $\log_2$ FC <-1, typically P <0.05) observed in severe and mild patient groups when compared with those of fatal patients, and almost all the significantly altered metabolites were down-regulated. These results indicate that the alterations of metabolite metabolism were more dramatic in fatal COVID-19 cases than in severe and mild ones who finally survived.

In addition, it is noteworthy that although the patients in both severe and mild

groups had met the hospital discharge criteria in the time points S2 and M2 as their COVID-19 nucleic acid tests turned negative twice consecutively, our metabolomic data clearly show that many of their metabolites had not returned to normal levels when compared with those in healthy volunteers (Figure 1B), indicating that these discharged patients had not been fully recovered from the impacts of this disease in physiology.

To further analyze the metabolomic data, the differentiated expressed metabolites (DEMs) were divided into those shared by all groups (F vs. H, S vs. H, and M vs. H) or those unique to the fatal group (F vs. H). Then, we performed Kyoto Encyclopedia of Genes and Genomes (KEGG) functional enrichment analysis to annotate the potential functional implication of these differently grouped DEMs (Figure 2). As shared by all the three symptomatic groups, DEMs were enriched in total 12 pathways and significantly enriched in 3 pathways including pyrimidine metabolism, fructose and mannose metabolism, and carbon metabolism (Figure 2A-B and Table S6).

On the other hand, in the case of the fatality group, DEMs were significantly enriched in 4 pathways, including thyroid hormone synthesis, thyroid hormone signaling, purine metabolism, and autoimmune thyroid (Figure 2C-D and Table S7), suggesting that the alterations in these pathways are associated with the progress and deterioration of COVID-19.

Plasma lipidomic alternations correspond to clinical symptoms of COVID-19

We analyzed the lipids in different courses of fatal COVID-19 patients (F1-F4) that underwent significant change [F4 vs. H, >1 $\log_2$ FC <-1, typically P <0.05]. Most

of the significantly changed lipids are up-regulated and a positive correlation between the alteration of lipids and the course of disease deterioration could be readily observed in the fatal patients (Figure 3A and Table S8). Lipid subclasses, DG, FAA, and TG, were identified in higher abundance in the fatality group (F vs. H), and the relative abundances of these lipids increased with the deterioration of the disease. Particularly, DG(16:0/20:2/0:0) exhibited the greatest $\log_2$ FC (+4.2) in DGs, and TG(14:0/22:1/22:3) exhibited the greatest $\log_2$ FC (+4.2) in all significantly altered TGs. The increases of DG, free fatty acid (FFA), and TG under pathological conditions have been previously reported. For instance, lipolysis of adipose tissue increases due to EBOV infection, which converts TG to FFA and DG, and also results in enhanced recycling of the fatty acids back into TGs (9).

Besides, we observed that PCs were gradually reduced over the course of COVID-19 fatalities. PCs are synthesized in the liver and are the only phospholipid necessary for lipoprotein (18); therefore, the COVID-19-associated decrease of PCs in the fatality group indicates hepatic impairments happened in the fatality group. Additionally, decreases in LPCs and PCs in blood plasma have been observed in sepsis, cancer, and Dengue infection (19-22).

We also analyzed the lipids in different courses of severe and mild COVID-19 patients (S1 and S2; M1 and M2) that underwent the significant change [S1 vs. H, >1 $\log_2$ FC <-1, typically P <0.05; M1 vs. H, >1 $\log_2$ FC <-1, typically P <0.05] (Figure 3B and Table S9). Similar to those of metabolites, the total numbers of significantly altered lipids (>1 $\log_2$ fold change (FC) <-1, typically P <0.05) in the severe and mild

groups (S1 vs H, S2 vs H, M1 vs. H, and M2 vs H) were similar, which are significantly less than the number of altered lipids in the fatality group, indicating that the alterations of lipid metabolism were much more dramatic in fatal COVID-19 patients than in survivors. Besides, for either severe or mild groups of patients, many of their lipids had not returned to normal before their discharge from hospital (Figure 3B, S2 vs H and M2 vs H), even though SARS-CoV-2 could not be detected and the major clinical signs had disappeared in these patients based on official discharge criteria. Obviously, like the observations of metabolomic alterations, these discharged patients, no matter if they had experienced severe or mild symptoms, had not been fully recovered from the aftermath of COVID-19 in the aspects of both metabolite and lipid metabolisms.

Furthermore, the differentiated expressed lipids (DEIs) were divided into those shared by all groups (F vs. H and S vs. H plus M vs. H) or those unique to the fatality group (F vs. H), and subsequently subjected to KEGG functional enrichment analysis. As shared by all the three symptomatic groups, DEIs were enriched in total 7 pathways and significantly enriched in 4 pathways, including phosphatidylinositol signaling system, long-term depression, leishmaniasis, and inositol phosphate metabolism (Figure 4A-B and Table S10). In the case of fatality group, DEIs were significantly enriched in 6 pathways, including retrograde endocannabinoid signaling, pathogenic Escherichia coli infection, Kaposi sarcoma-associated herpesvirus infection, glycosylphosphatidylinositol-anchor biosynthesis, glycerophospholipid metabolism and autophagy (Figure 4C-D and Table S11).

Biomarkers associated with COVID-19

We summarized 5 metabolites and 15 lipids altered significantly among COVID-19 patients and healthy people. All the 5 metabolites were significantly down-regulated in COVID-19 patient compared to those in healthy volunteers (Figure 5 and Table S12). On the other hand, 8 lipids were significantly down-regulated and 7 lipids were significantly up-regulated compared to those in the healthy group (Figure 6 and Table S12). Among them, L-malic acid and Glycerol 3-phosphate showed the greatest reduction when comparing the fatality patients with healthy volunteers, and also showed dramatic reduction in both severe and mild groups. L-malic acid has important physiological functions, as it can directly enter the circulation of tricarboxylic acid to participate in human metabolism. Besides, L-malic acid can accelerate metabolism of ammonia to lower ammonia concentration in liver and to protect liver (23, 24); therefore, the dramatic reduction of L-malic acid is consistent with the hepatic impairment associated with COVID-19. Moreover, L-malic acid has been found to protect endothelial cells of human blood vessels and resist damage to endothelial cells.

D-Xylulose 5-phosphate (Xu-5-P) is a metabolite of the hexose monophosphate pathway that mediates glycolysis, as well as fatty acid and triglyceride synthesis. Xu-5-P is the coordinating signal that both activates phosphofructokinase in glycolysis and promotes transcription of the genes for lipogenesis, the hexose monophosphate shunt, and glycolysis, and is required for de novo synthesis of fat and hepatic energy utilization (25-28). The reduction of Xu-5-P indicates the downregulation of glycolysis and lipogenesis, which is also a reflection of hepatic impairment.

Carbamoyl phosphate is an important intermediate metabolite involved in removing excess ammonia in the urea cycle (14, 15). This metabolite is the downstream product of CPSI in mitochondria of liver cells. The observed downregulation of carbamoyl phosphate levels is associated with the severity of COVID-19, as its level in the mild patients were affected in the least extent. Importantly, the dramatic reduction of carbamoyl phosphate is usually associated with urea cycle disorder, raising the concern about the possibility of hyperammonemia and hyperammonemia-associated liver failure in COVID-19 patients.

Besides, the reductions of dihydrouracil, an intermediate breakdown product of uracil and GMP (29), are proposed to be caused by the defects of human metabolism. Glycerol-3-phosphate is a conserved three-carbon sugar and an obligatory component of energy-producing reactions including glycolysis and glycerolipid biosynthesis (30). Moreover, Glycerol-3-phosphate is an important mobile regulator of systemic acquired resistance, which provides broad spectrum systemic immunity in response to pathogenic infections (31). These metabolites and lipids show good correlation with the progress and severity of COVID-19, and can therefore serve as potential blood biomarkers for this disease.

Discussion

The main purpose of this study was to generate a high-quality resource of metabolomic and lipidomic datasets associated with COVID-19 to help understand the pathogenesis of COVID-19.

For these COVID-19 patients, the metabolisms of main amino acids, nucleotides, organic acids and carbohydrates were significantly decreased. Meanwhile, the lipids involved in glycerol metabolism pathway were upregulated, which maintain the balance of the energy metabolites of the body and are beneficial to the energy required for viral replication, suggesting that SARS-CoV-2 probably hijacks cellular metabolism like many other viruses (32). And we hypothesize that the course of COVID-19 is closely associated with the alternations of host pyrimidine metabolic, purine metabolic, and glycerol phospholipid metabolic pathways.

Importantly, many of the altered metabolites and lipids, including the proposed biomarkers L-malic acid, Xu-5-P, Carbamoyl phosphate, Glycerol-3-phosphate, PC, LPC, etc., correlate well with the progress and severity of COVID-19 and are closely associated with hepatic functions. Moreover, the downregulations of L-malic acid and Carbamoyl phosphate probably cause the abnormal accumulation of ammonia (i.e. hyperammonemia), which may in turn result in disease deterioration. In addition, the metabolisms of purine and thyroid hormones were significantly altered in the fatality group. Purine metabolism mainly occurs in human liver, and the thyroid hormone can affect hepatic protein synthesis and glycogen decomposition. Therefore, our findings show that the development of COVID-19 can cause hepatic impairment in these

patients, which is consistent with the observations that a large number of COVID-19 patients showed liver function abnormalities (Table S13) (6).

Besides, our data show that the metabolic pathway of glycerophospholipids has been significantly changed, and glycerophospholipids are closely related with cardiovascular diseases. However, we did not find obvious pattern or significant difference of underlying diseases, such as hypertension, cardiac disease, diabetes, cerebrovascular disease, chronic hepatitis, and cancer, in the medical records of all the patient groups involved in this study. Therefore, this finding suggests that the fatality caused by COVID-19 might be related with cardiac impairment. Interestingly, COVID-19 has been recently reported to probably cause the loss of the smell and taste sense (https://www.npr.org/sections/goatsandsoda/2020/03/26/821582951/is-loss-of-smell-and-taste-a-symptom-of-covid-19-doctors-want-to-find-out), and the KEGG analysis also showed that the taste transduction pathway is affected.

The metabolomic and lipidomic analyses also show that, although the patients in both the severe and mild symptom groups had met the official hospital discharge criteria as their COVID-19 nucleic acid tests turned negative consecutively twice and major clinical signs disappeared, many of their fundamental metabolites and lipids failed to return to normal. This finding indicates that these discharged patients, regardless of the severity of their previous symptoms, had not been fully recovered from the disease in the aspect of metabolism, particularly hepatic functions. Therefore, even after the clearance of SARS-CoV-2 from patient bodies, these convalescent COVID-19 patients

still need better nutrition and care that would be very helpful for their faster and full recovery from the disease.

The metabolomic and lipidomic alterations in patient plasma mainly reflect the systematic responses of the metabolisms of diverse cell types and organ systems that were affected by COVID-19. Therefore, the interpretations of the datasets should be integrated with other types of system studies, such as the transcriptome and proteome of specific tissue and body fluid samples, as well as clinical observations and laboratory examinations, to have a clearer and more comprehensive picture of the development of this disease. Moreover, such an integration would help us better understand the impacts of COVID-19 to specific cells and/or tissues infected by SARS-CoV-2.

In summary, the metabolomic and lipidomic datasets of the cohort of COVID-19 patients under different symptomatic conditions are highly valuable resources for better understanding the host metabolic responses associated with COVID-19, which expands our knowledge about the pathogenesis of COVID-19, accelerates identification of disease biomarkers and development of diagnostic assays, and provides hints of potential therapeutic strategies.

Author contributions

D.W., T.S., X.Y. and J.-X.S. performed experiments with the help of W.L., M.H., Y.Y., Q.Y., T.Z., J.X., Y.W., J.M., H.W., T.T., Y.R. Y.W.; M.Z. analyzed the metabolomics and lipidomics data with the help of D.W. and Y.Q.; Y.Q., D.-Y.Z., Y.S. and X.Z. performed the experimental design and data interpretation; X.Z, Y.Q., Y.S., and D.-Y.Z. designed the overall study, analyzed the data, and wrote the paper.

Competing Interests statement

The authors declare no conflicts of interest.

Acknowledgments

We thank the patients, and the nurses and clinical staffs who are providing care for these patients. We thank the helpful discussions with Drs. Yan Wang and Yong Liu at Wuhan University. We also thank many staff members at Wuhan Jinyintan Hospital and Wuhan Metware Biotechnology Co., Ltd. for their contributions and assistance in this study. We sincerely pay tribute to our colleagues who are striving in the forefront of taking care of COVID-19 patients and studying this novel coronavirus in Wuhan and other places around the world.

This work was supported by the Strategic Priority Research Program of CAS (XDB29010300 to X.Z.), the National Science and Technology Major Project (2020ZX09201-001 to D.-Y.Z, and 2018ZX10101004 to X.Z.), and National Natural Science Foundation of China (81873964 to Y.Q., and 31670161 to X.Z.).

References

1. The Novel Coronavirus Pneumonia Emergency Response Epidemiology, T. The Epidemiological Characteristics of an Outbreak of 2019 Novel Coronavirus Diseases (COVID-19) — China, 2020. *China CDC Weekly*. 2020; **2**(8): 113-22.

2. WHO. Coronavirus disease 2019 (COVID-19) Situation Report - 71. *https://wwwwhoint/docs/default-source/coronaviruse/situation-reports/20200331-sitrep-71-covid-19pdf?sfvrsn=4360e92b_4 (accessed March 31, 2020)*. 2020.

3. Wang, D, Hu, B, Hu, C*, et al.* Clinical Characteristics of 138 Hospitalized Patients With 2019 Novel Coronavirus-Infected Pneumonia in Wuhan, China. *JAMA*. 2020.

4. Huang, C, Wang, Y, Li, X*, et al.* Clinical features of patients infected with 2019 novel coronavirus in Wuhan, China. *Lancet*. 2020.

5. Chen, N, Zhou, M, Dong, X*, et al.* Epidemiological and clinical characteristics of 99 cases of 2019 novel coronavirus pneumonia in Wuhan, China: a descriptive study. *Lancet*. 2020.

6. Zhang, C, Shi, L, Wang, FS. Liver injury in COVID-19: management and challenges. *Lancet Gastroenterol Hepatol*. 2020.

7. Yang, X, Yu, Y, Xu, J*, et al.* Clinical course and outcomes of critically ill patients with SARS-CoV-2 pneumonia in Wuhan, China: a single-centered, retrospective, observational study. *The Lancet Respiratory Medicine*. 2020.

8. Eisfeld, AJ, Halfmann, PJ, Wendler, JP*, et al.* Multi-platform 'Omics Analysis of Human Ebola Virus Disease Pathogenesis. *Cell Host Microbe*. 2017; **22**(6): 817-29 e8.

9. Kyle, JE, Burnum-Johnson, KE, Wendler, JP*, et al.* Plasma lipidome reveals critical illness and recovery from human Ebola virus disease. *Proc Natl Acad Sci U S A*. 2019; **116**(9): 3919-28.

10. National Health Commission of China, T. National Health Commission of China. *New coronavirus pneumonia prevention and control program (6th edn) http://wwwnhcgovcn/yzygj/s7653p/202002/8334a8326dd94d329df351d7da8aefc2/files/b218cfeb1bc54639af227f922bf6b817pdf (accessed Feb 18, 2020; in Chinese)*. 2020.

11. Soeters, PB, Grecu, I. Have we enough glutamine and how does it work? A clinician's view. *Ann Nutr Metab*. 2012; **60**(1): 17-26.

12. Lopez-Cruz, RI, Crocker, DE, Gaxiola-Robles, R*, et al.* Plasma Hypoxanthine-Guanine Phosphoribosyl Transferase Activity in Bottlenose Dolphins Contributes to Avoiding Accumulation of Non-recyclable Purines. *Front Physiol*. 2016; **7**: 213.

13. Auler, K, Broock, R, Nyhan, WL. Determination of Activity of the Enzymes Hypoxanthine Phosphoribosyl Transferase (HPRT) and Adenine Phosphoribosyl Transferase (APRT) in Blood Spots on Filter Paper. *Curr Protoc Hum Genet*. 2015; **86**: 17 9 1- 9 0.

14. Sigoillot, FD, Kotsis, DH, Serre, V*, et al.* Nuclear localization and mitogen-activated protein kinase phosphorylation of the multifunctional protein CAD. *J Biol Chem*. 2005; **280**(27): 25611-20.

15. Struck, J, Uhlein, M, Morgenthaler, NG*, et al.* Release of the mitochondrial enzyme carbamoyl phosphate synthase under septic conditions. *Shock*. 2005; **23**(6): 533-8.

16. Schnater, JM, Bruder, E, Bertschin, S*, et al.* Subcutaneous and intrahepatic growth of human hepatoblastoma in immunodeficient mice. *J Hepatol*. 2006; **45**(3): 377-86.

17. Chen, KF, Lai, YY, Sun, HS*, et al.* Transcriptional repression of human cad gene by hypoxia inducible factor-1alpha. *Nucleic Acids Res*. 2005; **33**(16): 5190-8.

18. Cole, LK, Vance, JE, Vance, DE. Phosphatidylcholine biosynthesis and lipoprotein metabolism.

Biochim Biophys Acta. 2012; **1821**(5): 754-61.
19. Cui, L, Lee, YH, Kumar, Y*, et al.* Serum metabolome and lipidome changes in adult patients with primary dengue infection. *PLoS Negl Trop Dis*. 2013; **7**(8): e2373.
20. Ferrario, M, Cambiaghi, A, Brunelli, L*, et al.* Mortality prediction in patients with severe septic shock: a pilot study using a target metabolomics approach. *Sci Rep*. 2016; **6**: 20391.
21. Park, DW, Kwak, DS, Park, YY*, et al.* Impact of serial measurements of lysophosphatidylcholine on 28-day mortality prediction in patients admitted to the intensive care unit with severe sepsis or septic shock. *J Crit Care*. 2014; **29**(5): 882 e5-11.
22. Taylor, LA, Arends, J, Hodina, AK*, et al.* Plasma lyso-phosphatidylcholine concentration is decreased in cancer patients with weight loss and activated inflammatory status. *Lipids Health Dis*. 2007; **6**: 17.
23. Chi, Z, Wang, ZP, Wang, GY*, et al.* Microbial biosynthesis and secretion of l-malic acid and its applications. *Crit Rev Biotechnol*. 2016; **36**(1): 99-107.
24. Qiang, F. Effect of Malate-oligosaccharide Solution on Antioxidant Capacity of Endurance Athletes. *Open Biomed Eng J*. 2015; **9**: 326-9.
25. Veech, RL. A humble hexose monophosphate pathway metabolite regulates short- and long-term control of lipogenesis. *Proc Natl Acad Sci U S A*. 2003; **100**(10): 5578-80.
26. Shaeri, J, Wright, I, Rathbone, EB*, et al.* Characterization of enzymatic D-xylulose 5-phosphate synthesis. *Biotechnol Bioeng*. 2008; **101**(4): 761-7.
27. Nakayama, Y, Kinoshita, A, Tomita, M. Dynamic simulation of red blood cell metabolism and its application to the analysis of a pathological condition. *Theor Biol Med Model*. 2005; **2**: 18.
28. Kabashima, T, Kawaguchi, T, Wadzinski, BE*, et al.* Xylulose 5-phosphate mediates glucose-induced lipogenesis by xylulose 5-phosphate-activated protein phosphatase in rat liver. *Proc Natl Acad Sci U S A*. 2003; **100**(9): 5107-12.
29. Jacobs, BAW, Snoeren, N, Samim, M*, et al.* The impact of liver resection on the dihydrouracil:uracil plasma ratio in patients with colorectal liver metastases. *Eur J Clin Pharmacol*. 2018; **74**(6): 737-44.
30. Glycerol-3-phosphate cytidylyltransferase. In: Schomburg, D, Schomburg, I, Chang, A (eds.). *Springer Handbook of Enzymes*. Berlin, Heidelberg: Springer Berlin Heidelberg; 2007. 404-11.
31. Chanda, B, Xia, Y, Mandal, MK*, et al.* Glycerol-3-phosphate is a critical mobile inducer of systemic immunity in plants. *Nat Genet*. 2011; **43**(5): 421-7.
32. Thaker, SK, Ch'ng, J, Christofk, HR. Viral hijacking of cellular metabolism. *BMC Biol*. 2019; **17**(1): 59.

Figure legends

Figure 1. COVID-19 signatures in the plasma metabolome. Selected average plasma metabolite expression levels and associated *p* values for COVID-19 fatality patient group vs. healthy volunteer group (A), and severe or mild vs. healthy groups (B). F, fatalities, first, second, third and fourth samples, F1, F2, F3 and F4. S, severe patients, first and second samples, S1 and S2; M, mild patients, first and second samples, M1 and M2.

Figure 2. The metabolome KEGG enrichment analysis of COVID-19 patient plasma. (A-B) KEGG pathway analysis of DEMs shared in all the groups. The color of bubbles represents the value of adjusted *P* value, and the size of bubbles represents the number of counts (sorted by gene ratio). (C-D) KEGG pathway analysis of DEMs shared unique to the fatal groups.

Figure 3. COVID-19 signatures in the plasma lipidome. Selected average plasma lipid expression levels and associated p values for COVID-19 fatality group vs. healthy volunteer group (A), and severe or mild vs. healthy groups (B). AA, arachidonic acid; BA, bile acid; CAR, carnitine; CE, cholesterol ester; Cer, ceramide; DG, diacylglycerides; TG, Triglycerides; FA, fatty acid; FFA, free fatty acids; LPA, lysophosphatidic acid; PC, phosphatidylcholine; LPC, lysophosphatidylcholine; PE, phosphatidylethanolamine; LPE, lysophosphatidyl ethanolamine; LPG, lysophosphatidylglycerol; PI, phosphatidylinositol; PS, phosphatidylserine; LPO, lipid

peroxide.

Figure 4. The lipidome KEGG enrichment analysis of COVID-19 patients. (A-B) KEGG pathway analysis of DEIs shared in all the groups. The color of bubbles represents the value of adjusted *P* value, and the size of bubbles represents the number of counts (sorted by gene ratio). (C-D) KEGG pathway analysis of DEIs shared unique to the fatal groups.

Figure 5. The potential metabolomic biomarkers of COVID-19. The normalized expression for each metabolite. Each dot represents a single patient sample, and each patient group is differently colored as indicated. F, fatalities; S, the patients with severe symptom; M, the patients with mild symptom; H, healthy volunteers. *$P<0.05$, **$P<0.01$.

Figure 6. The potential lipidomic biomarkers of COVID-19. The normalized expression for each lipid. Each dot represents a single patient sample, and each patient group is differently colored as indicated. F, fatalities; S, the patients with severe symptom; M, the patients with mild symptom; H, healthy volunteers. *$P<0.05$, **$P<0.01$.

Figure 1

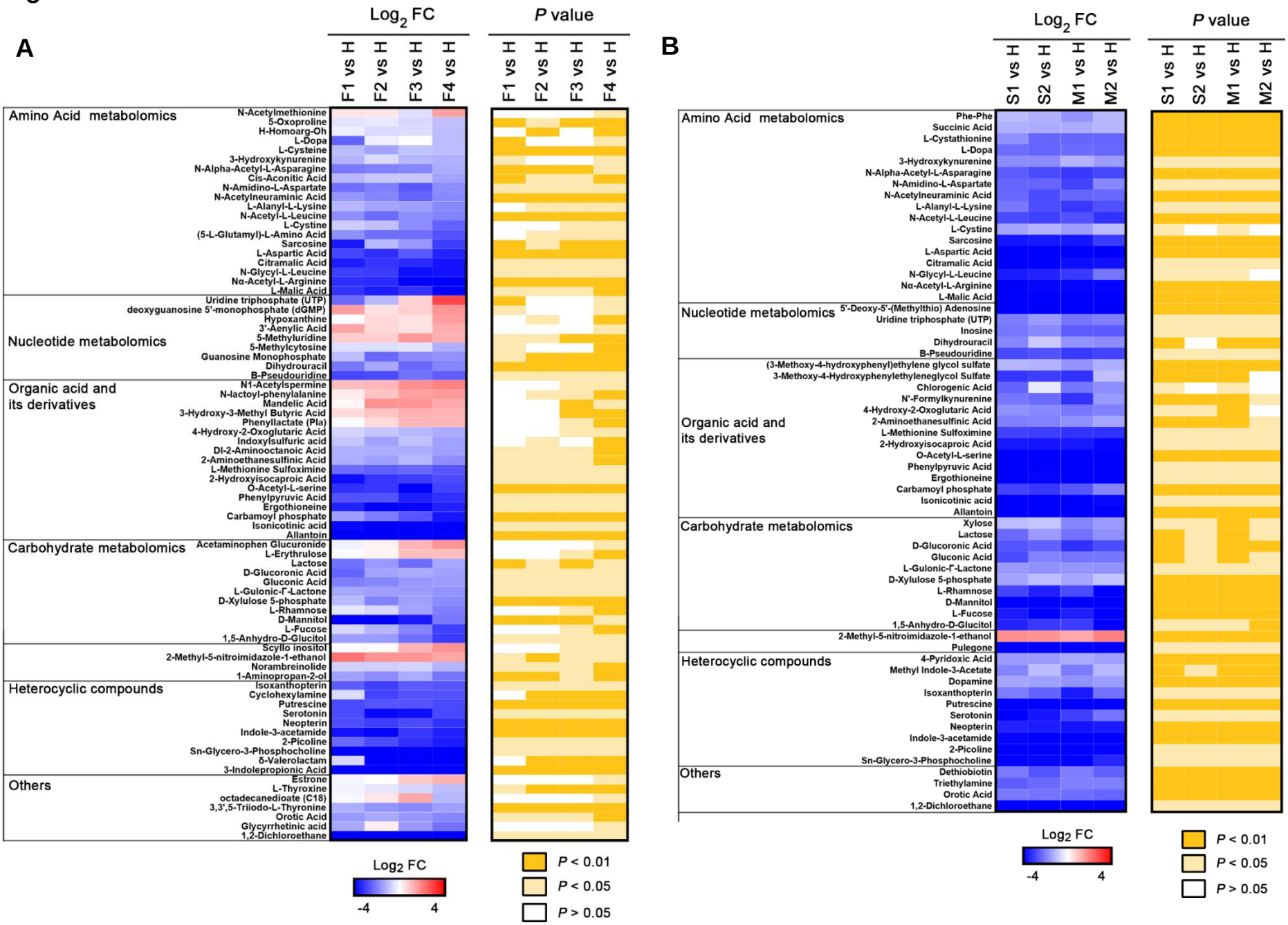
A
Log2 FC
P value
F1 vs H
F2 vs H
F3 vs H
F4 vs H
Amino Acid metabolomics
N-Acetylmethionine
5-Oxoproline
H-Homoarg-Oh
L-Dopa
L-Cysteine
3-Hydroxykynurenine
N-Alpha-Acetyl-L-Asparagine
Cis-Aconitic Acid
N-Amidino-L-Aspartate
N-Acetylneuraminic Acid
L-Alanyl-L-Lysine
N-Acetyl-L-Leucine
L-Cystine
(5-L-Glutamyl)-L-Amino Acid
Sarcosine
L-Aspartic Acid
Citramalic Acid
N-Glycyl-L-Leucine
Nα-Acetyl-L-Arginine
L-Malic Acid
Nucleotide metabolomics
Uridine triphosphate (UTP)
deoxyguanosine 5'-monophosphate (dGMP)
Hypoxanthine
3'-Aenylic Acid
5-Methyluridine
5-Methylcytosine
Guanosine Monophosphate
Dihydrouracil
B-Pseudouridine
Organic acid and its derivatives
N1-Acetylspermine
N-lactoyl-phenylalanine
Mandelic Acid
3-Hydroxy-3-Methyl Butyric Acid
Phenyllactate (Pla)
4-Hydroxy-2-Oxoglutaric Acid
Indoxylsulfuric acid
Dl-2-Aminooctanoic Acid
2-Aminoethanesulfinic Acid
L-Methionine Sulfoximine
2-Hydroxyisocaproic Acid
O-Acetyl-L-serine
Phenylpyruvic Acid
Ergothioneine
Carbamoyl phosphate
Isonicotinic acid
Allantoin
Carbohydrate metabolomics
Acetaminophen Glucuronide
L-Erythrulose
Lactose
D-Glucoronic Acid
Gluconic Acid
L-Gulonic-Γ-Lactone
D-Xylulose 5-phosphate
L-Rhamnose
D-Mannitol
L-Fucose
1,5-Anhydro-D-Glucitol
Scyllo inositol
2-Methyl-5-nitroimidazole-1-ethanol
Norambreinolide
1-Aminopropan-2-ol
Heterocyclic compounds
Isoxanthopterin
Cyclohexylamine
Putrescine
Serotonin
Neopterin
Indole-3-acetamide
2-Picoline
Sn-Glycero-3-Phosphocholine
δ-Valerolactam
3-Indolepropionic Acid
Others
Estrone
L-Thyroxine
octadecanedioate (C18)
3,3',5-Triiodo-L-Thyronine
Orotic Acid
Glycyrrhetinic acid
1,2-Dichloroethane
Log2 FC
-4
4
P < 0.01
P < 0.05
P > 0.05
B
Log2 FC
P value
S1 vs H
S2 vs H
M1 vs H
M2 vs H
Amino Acid metabolomics
Phe-Phe
Succinic Acid
L-Cystathionine
L-Dopa
3-Hydroxykynurenine
N-Alpha-Acetyl-L-Asparagine
N-Amidino-L-Aspartate
N-Acetylneuraminic Acid
L-Alanyl-L-Lysine
N-Acetyl-L-Leucine
L-Cystine
Sarcosine
L-Aspartic Acid
Citramalic Acid
N-Glycyl-L-Leucine
Nα-Acetyl-L-Arginine
L-Malic Acid
Nucleotide metabolomics
5'-Deoxy-5'-(Methylthio) Adenosine
Uridine triphosphate (UTP)
Inosine
Dihydrouracil
B-Pseudouridine
Organic acid and its derivatives
(3-Methoxy-4-hydroxyphenyl)ethylene glycol sulfate
3-Methoxy-4-Hydroxyphenylethyleneglycol Sulfate
Chlorogenic Acid
N'-Formylkynurenine
4-Hydroxy-2-Oxoglutaric Acid
2-Aminoethanesulfinic Acid
L-Methionine Sulfoximine
2-Hydroxyisocaproic Acid
O-Acetyl-L-serine
Phenylpyruvic Acid
Ergothioneine
Carbamoyl phosphate
Isonicotinic acid
Allantoin
Carbohydrate metabolomics
Xylose
Lactose
D-Glucoronic Acid
Gluconic Acid
L-Gulonic-Γ-Lactone
D-Xylulose 5-phosphate
L-Rhamnose
D-Mannitol
L-Fucose
1,5-Anhydro-D-Glucitol
2-Methyl-5-nitroimidazole-1-ethanol
Pulegone
Heterocyclic compounds
4-Pyridoxic Acid
Methyl Indole-3-Acetate
Dopamine
Isoxanthopterin
Putrescine
Serotonin
Neopterin
Indole-3-acetamide
2-Picoline
Sn-Glycero-3-Phosphocholine
Others
Dethiobiotin
Triethylamine
Orotic Acid
1,2-Dichloroethane
Log2 FC
-4
4
P < 0.01
P < 0.05
P > 0.05

Figure 2

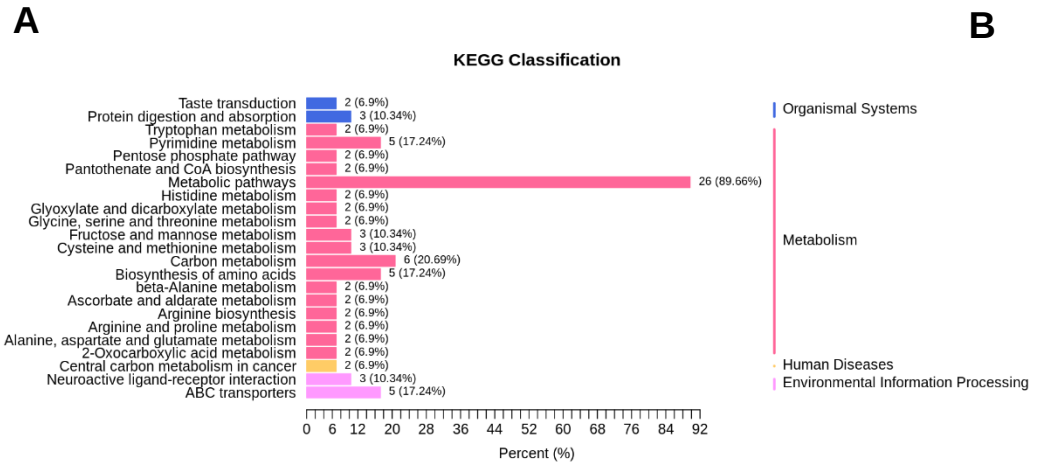
A
KEGG Classification
Taste transduction
Protein digestion and absorption
Tryptophan metabolism
Pyrimidine metabolism
Pentose phosphate pathway
Pantothenate and CoA biosynthesis
Metabolic pathways
Histidine metabolism
Glyoxylate and dicarboxylate metabolism
Glycine, serine and threonine metabolism
Fructose and mannose metabolism
Cysteine and methionine metabolism
Carbon metabolism
Biosynthesis of amino acids
beta-Alanine metabolism
Ascorbate and aldarate metabolism
Arginine biosynthesis
Arginine and proline metabolism
Alanine, aspartate and glutamate metabolism
2-Oxocarboxylic acid metabolism
Central carbon metabolism in cancer
Neuroactive ligand-receptor interaction
ABC transporters
2 (6.9%)
3 (10.34%)
2 (6.9%)
5 (17.24%)
2 (6.9%)
2 (6.9%)
26 (89.66%)
2 (6.9%)
2 (6.9%)
2 (6.9%)
3 (10.34%)
3 (10.34%)
6 (20.69%)
5 (17.24%)
2 (6.9%)
2 (6.9%)
2 (6.9%)
2 (6.9%)
2 (6.9%)
2 (6.9%)
2 (6.9%)
2 (6.9%)
3 (10.34%)
5 (17.24%)
0 6 12 20 28 36 44 52 60 68 76 84 92
Percent (%)
Organismal Systems
Metabolism
Human Diseases
Environmental Information Processing

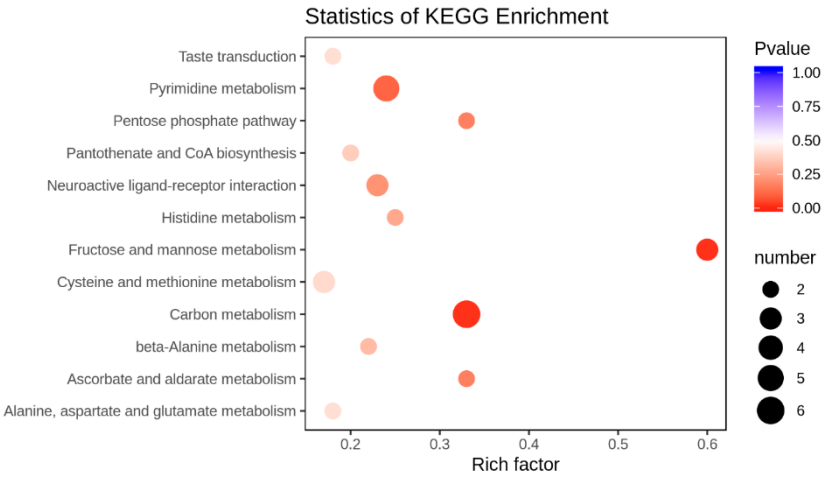
B
Statistics of KEGG Enrichment
Taste transduction
Pyrimidine metabolism
Pentose phosphate pathway
Pantothenate and CoA biosynthesis
Neuroactive ligand-receptor interaction
Histidine metabolism
Fructose and mannose metabolism
Cysteine and methionine metabolism
Carbon metabolism
beta-Alanine metabolism
Ascorbate and aldarate metabolism
Alanine, aspartate and glutamate metabolism
0.2 0.3 0.4 0.5 0.6
Rich factor
Pvalue
1.00 0.75 0.50 0.25 0.00
number
2 3 4 5 6

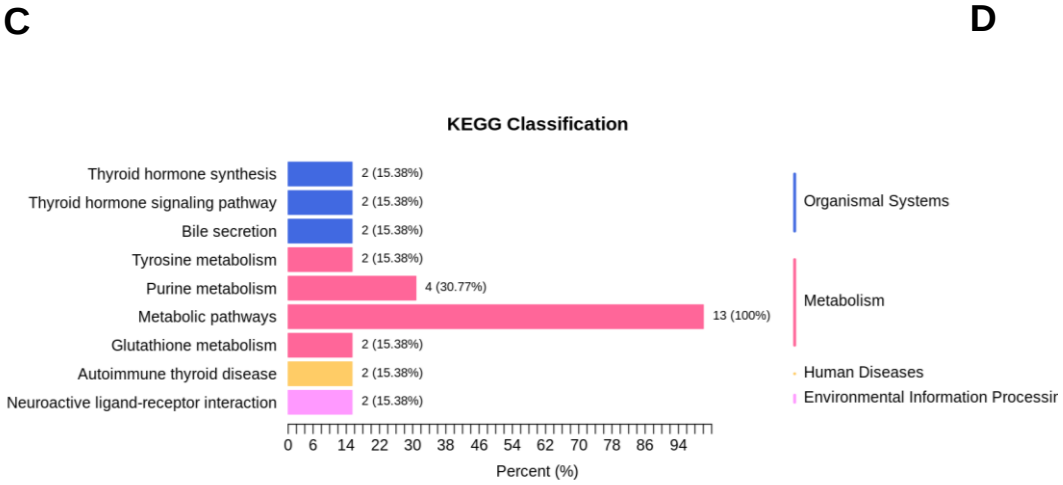
C
KEGG Classification
Thyroid hormone synthesis
Thyroid hormone signaling pathway
Bile secretion
Tyrosine metabolism
Purine metabolism
Metabolic pathways
Glutathione metabolism
Autoimmune thyroid disease
Neuroactive ligand-receptor interaction
2 (15.38%)
2 (15.38%)
2 (15.38%)
2 (15.38%)
4 (30.77%)
13 (100%)
2 (15.38%)
2 (15.38%)
2 (15.38%)
0 6 14 22 30 38 46 54 62 70 78 86 94
Percent (%)
Organismal Systems
Metabolism
Human Diseases
Environmental Information Processir

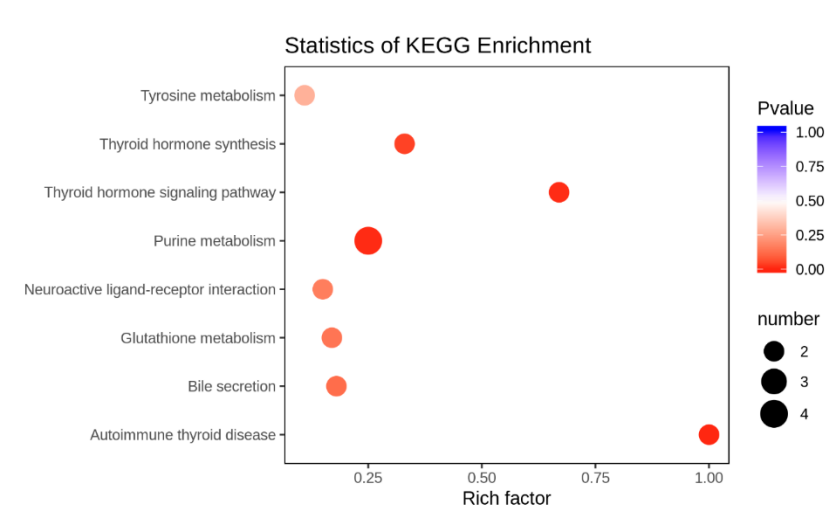
D
Statistics of KEGG Enrichment
Tyrosine metabolism
Thyroid hormone synthesis
Thyroid hormone signaling pathway
Purine metabolism
Neuroactive ligand-receptor interaction
Glutathione metabolism
Bile secretion
Autoimmune thyroid disease
0.25 0.50 0.75 1.00
Rich factor
Pvalue
1.00 0.75 0.50 0.25 0.00
number
2 3 4

Figure 3

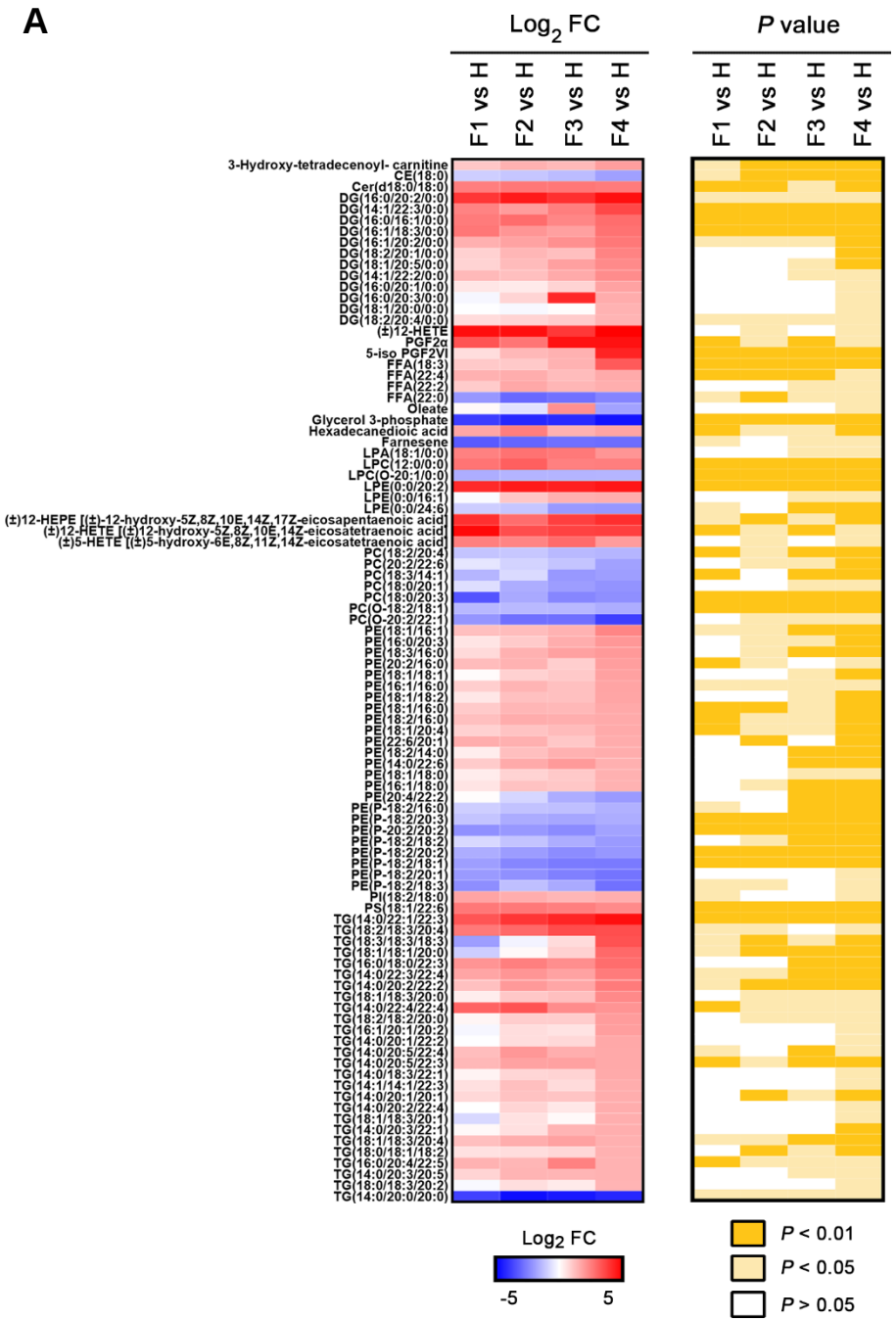
A
Log2 FC
P value
F1 vs H
F2 vs H
F3 vs H
F4 vs H
3-Hydroxy-tetradecenoyl- carnitine
CE(18:0)
Cer(d18:0/18:0)
DG(16:0/20:2/0:0)
DG(14:1/22:3/0:0)
DG(16:0/16:1/0:0)
DG(16:1/18:3/0:0)
DG(16:1/20:2/0:0)
DG(18:2/20:1/0:0)
DG(18:1/20:5/0:0)
DG(14:1/22:2/0:0)
DG(16:0/20:1/0:0)
DG(16:0/20:3/0:0)
DG(18:1/20:0/0:0)
DG(18:2/20:4/0:0)
(±)12-HETE
PGF2α
5-iso PGF2VI
FFA(18:3)
FFA(22:4)
FFA(22:2)
FFA(22:0)
Oleate
Glycerol 3-phosphate
Hexadecanedioic acid
Farnesene
LPA(18:1/0:0)
LPC(12:0/0:0)
LPC(O-20:1/0:0)
LPE(0:0/20:2)
LPE(0:0/16:1)
LPE(0:0/24:6)
(±)12-HEPE [(±)-12-hydroxy-5Z,8Z,10E,14Z,17Z-eicosapentaenoic acid]
(±)12-HETE [(±)12-hydroxy-5Z,8Z,10E,14Z-eicosatetraenoic acid]
(±)5-HETE [(±)5-hydroxy-6E,8Z,11Z,14Z-eicosatetraenoic acid]
PC(18:2/20:4)
PC(20:2/22:6)
PC(18:3/14:1)
PC(18:0/20:1)
PC(18:0/20:3)
PC(O-18:2/18:1)
PC(O-20:2/22:1)
PE(18:1/16:1)
PE(16:0/20:3)
PE(18:3/16:0)
PE(20:2/16:0)
PE(18:1/18:1)
PE(16:1/16:0)
PE(18:1/18:2)
PE(18:1/16:0)
PE(18:2/16:0)
PE(18:1/20:4)
PE(22:6/20:1)
PE(18:2/14:0)
PE(14:0/22:6)
PE(18:1/18:0)
PE(16:1/18:0)
PE(20:4/22:2)
PE(P-18:2/16:0)
PE(P-18:2/20:3)
PE(P-20:2/20:2)
PE(P-18:2/18:2)
PE(P-18:2/20:2)
PE(P-18:2/18:1)
PE(P-18:2/20:1)
PE(P-18:2/18:3)
PI(18:2/18:0)
PS(18:1/22:6)
TG(14:0/22:1/22:3)
TG(18:2/18:3/20:4)
TG(18:3/18:3/18:3)
TG(18:1/18:1/20:0)
TG(16:0/18:0/22:3)
TG(14:0/22:3/22:4)
TG(14:0/20:2/22:2)
TG(18:1/18:3/20:0)
TG(14:0/22:4/22:4)
TG(18:2/18:2/20:0)
TG(16:1/20:1/20:2)
TG(14:0/20:1/22:2)
TG(14:0/20:5/22:4)
TG(14:0/20:5/22:3)
TG(14:0/18:3/22:1)
TG(14:1/14:1/22:3)
TG(14:0/20:1/20:1)
TG(14:0/20:2/22:4)
TG(18:1/18:3/20:1)
TG(14:0/20:3/22:1)
TG(18:1/18:3/20:4)
TG(18:0/18:1/18:2)
TG(16:0/20:4/22:5)
TG(14:0/20:3/20:5)
TG(18:0/18:3/20:2)
TG(14:0/20:0/20:0)
Log2 FC
-5
5
P < 0.01
P < 0.05
P > 0.05

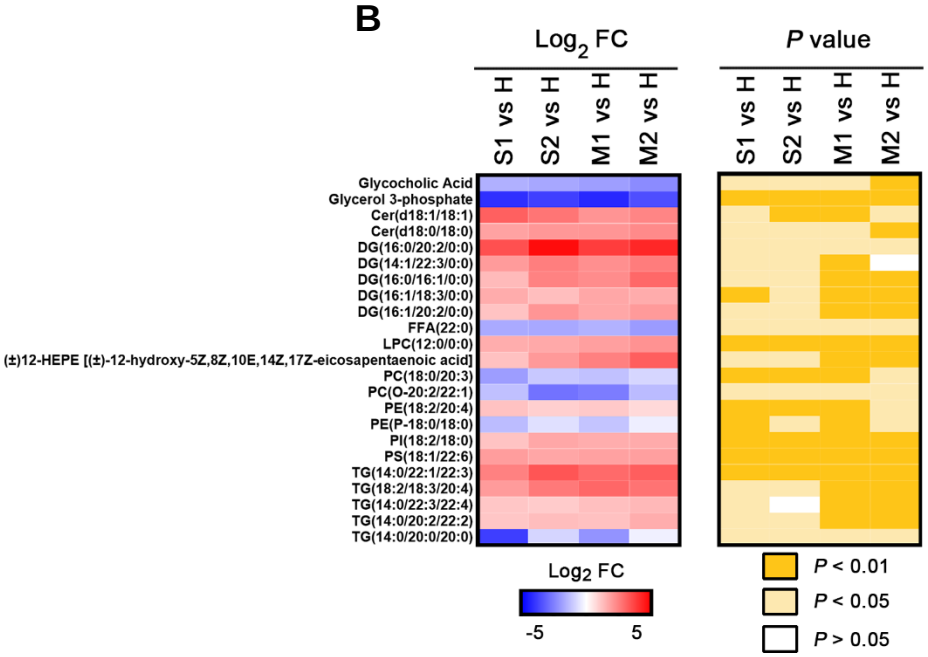
B
Log2 FC
P value
S1 vs H
S2 vs H
M1 vs H
M2 vs H
Glycocholic Acid
Glycerol 3-phosphate
Cer(d18:1/18:1)
Cer(d18:0/18:0)
DG(16:0/20:2/0:0)
DG(14:1/22:3/0:0)
DG(16:0/16:1/0:0)
DG(16:1/18:3/0:0)
DG(16:1/20:2/0:0)
FFA(22:0)
LPC(12:0/0:0)
(±)12-HEPE [(±)-12-hydroxy-5Z,8Z,10E,14Z,17Z-eicosapentaenoic acid]
PC(18:0/20:3)
PC(O-20:2/22:1)
PE(18:2/20:4)
PE(P-18:0/18:0)
PI(18:2/18:0)
PS(18:1/22:6)
TG(14:0/22:1/22:3)
TG(18:2/18:3/20:4)
TG(14:0/22:3/22:4)
TG(14:0/20:2/22:2)
TG(14:0/20:0/20:0)
Log2 FC
-5
5
P < 0.01
P < 0.05
P > 0.05

Figure 4

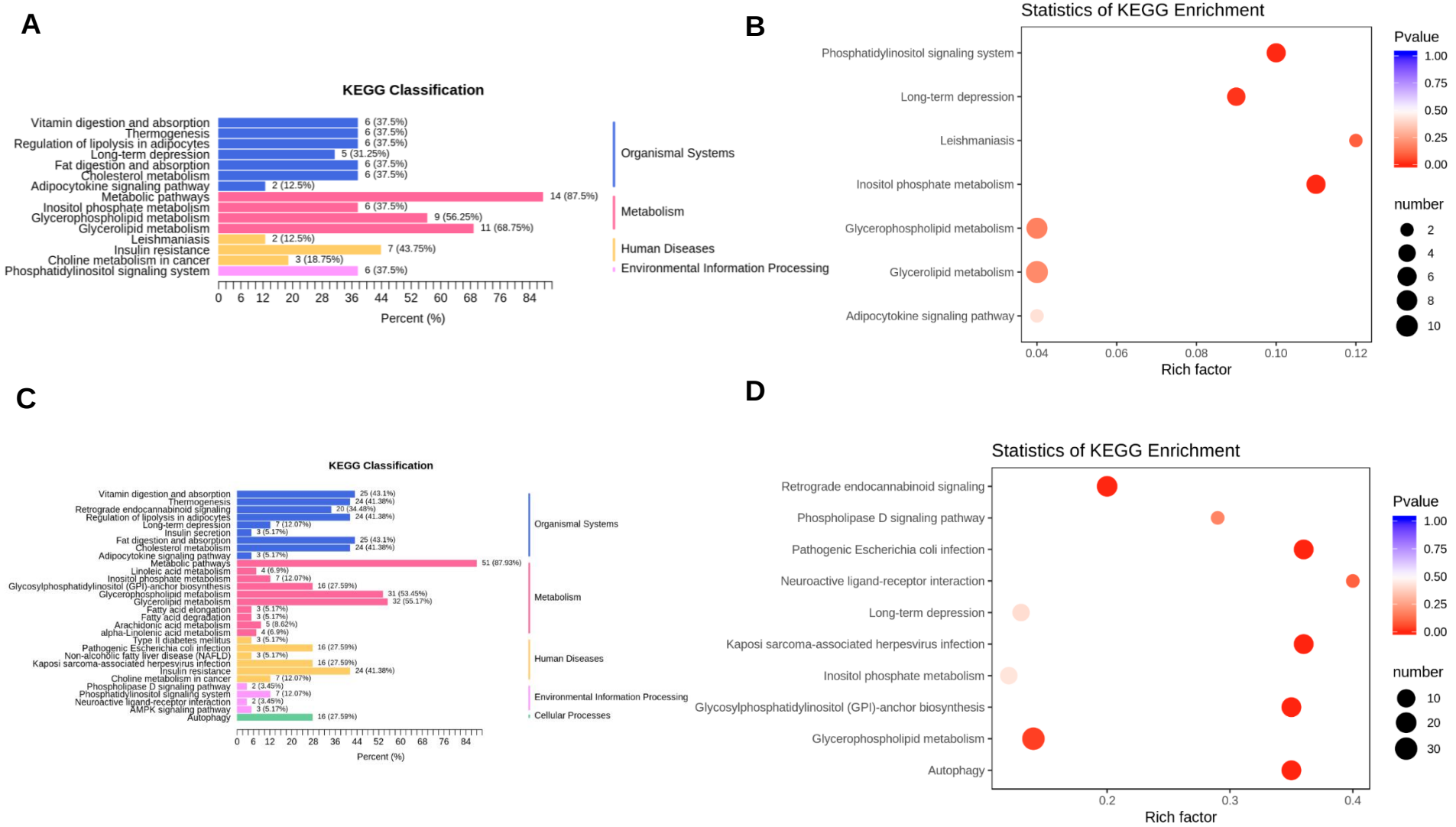
A
KEGG Classification
Vitamin digestion and absorption
Thermogenesis
Regulation of lipolysis in adipocytes
Long-term depression
Fat digestion and absorption
Cholesterol metabolism
Adipocytokine signaling pathway
Metabolic pathways
Inositol phosphate metabolism
Glycerophospholipid metabolism
Glycerolipid metabolism
Leishmaniasis
Insulin resistance
Choline metabolism in cancer
Phosphatidylinositol signaling system
6 (37.5%)
6 (37.5%)
6 (37.5%)
5 (31.25%)
6 (37.5%)
6 (37.5%)
2 (12.5%)
14 (87.5%)
6 (37.5%)
9 (56.25%)
11 (68.75%)
2 (12.5%)
7 (43.75%)
3 (18.75%)
6 (37.5%)
0 6 12 20 28 36 44 52 60 68 76 84
Percent (%)
Organismal Systems
Metabolism
Human Diseases
Environmental Information Processing
B
Statistics of KEGG Enrichment
Phosphatidylinositol signaling system
Long-term depression
Leishmaniasis
Inositol phosphate metabolism
Glycerophospholipid metabolism
Glycerolipid metabolism
Adipocytokine signaling pathway
0.04 0.06 0.08 0.10 0.12
Rich factor
Pvalue
1.00 0.75 0.50 0.25 0.00
number
2 4 6 8 10
C
KEGG Classification
Vitamin digestion and absorption
Thermogenesis
Retrograde endocannabinoid signaling
Regulation of lipolysis in adipocytes
Long-term depression
Insulin secretion
Fat digestion and absorption
Cholesterol metabolism
Adipocytokine signaling pathway
Metabolic pathways
Linoleic acid metabolism
Inositol phosphate metabolism
Glycosylphosphatidylinositol (GPI)-anchor biosynthesis
Glycerophospholipid metabolism
Glycerolipid metabolism
Fatty acid elongation
Fatty acid degradation
Arachidonic acid metabolism
alpha-Linolenic acid metabolism
Type II diabetes mellitus
Pathogenic Escherichia coli infection
Non-alcoholic fatty liver disease (NAFLD)
Kaposi sarcoma-associated herpesvirus infection
Insulin resistance
Choline metabolism in cancer
Phospholipase D signaling pathway
Phosphatidylinositol signaling system
Neuroactive ligand-receptor interaction
AMPK signaling pathway
Autophagy
25 (43.1%)
24 (41.38%)
20 (34.48%)
24 (41.38%)
7 (12.07%)
3 (5.17%)
25 (43.1%)
24 (41.38%)
3 (5.17%)
51 (87.93%)
4 (6.9%)
7 (12.07%)
16 (27.59%)
31 (53.45%)
32 (55.17%)
3 (5.17%)
3 (5.17%)
5 (8.62%)
4 (6.9%)
3 (5.17%)
16 (27.59%)
3 (5.17%)
16 (27.59%)
24 (41.38%)
7 (12.07%)
2 (3.45%)
7 (12.07%)
2 (3.45%)
3 (5.17%)
16 (27.59%)
0 6 12 20 28 36 44 52 60 68 76 84
Percent (%)
Organismal Systems
Metabolism
Human Diseases
Environmental Information Processing
Cellular Processes
D
Statistics of KEGG Enrichment
Retrograde endocannabinoid signaling
Phospholipase D signaling pathway
Pathogenic Escherichia coli infection
Neuroactive ligand-receptor interaction
Long-term depression
Kaposi sarcoma-associated herpesvirus infection
Inositol phosphate metabolism
Glycosylphosphatidylinositol (GPI)-anchor biosynthesis
Glycerophospholipid metabolism
Autophagy
0.2 0.3 0.4
Rich factor
Pvalue
1.00 0.75 0.50 0.25 0.00
number
10 20 30

Figure 5

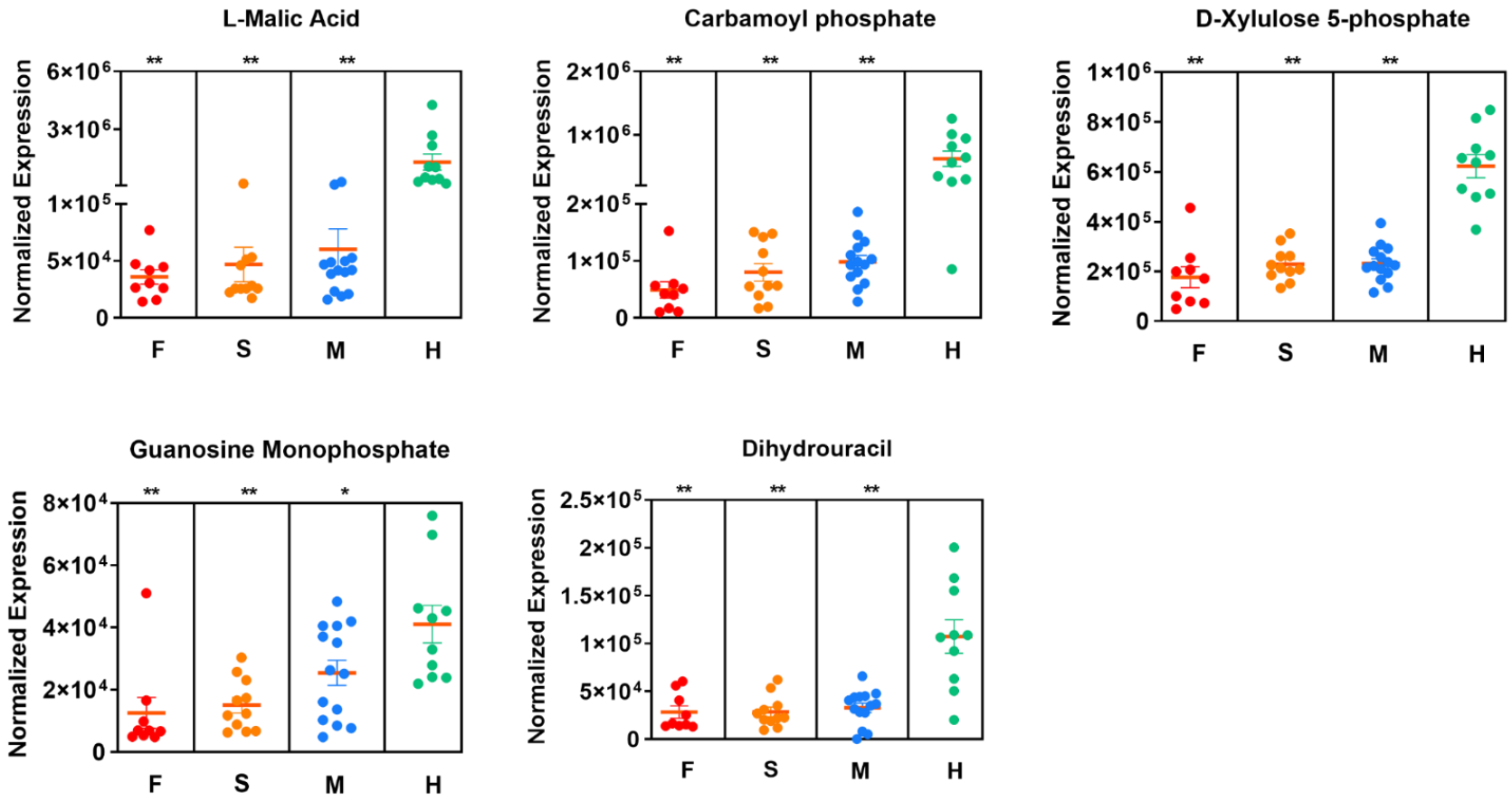
L-Malic Acid
Carbamoyl phosphate
D-Xylulose 5-phosphate
Guanosine Monophosphate
Dihydrouracil
Normalized Expression
F
S
M
H
**
*

Figure 6

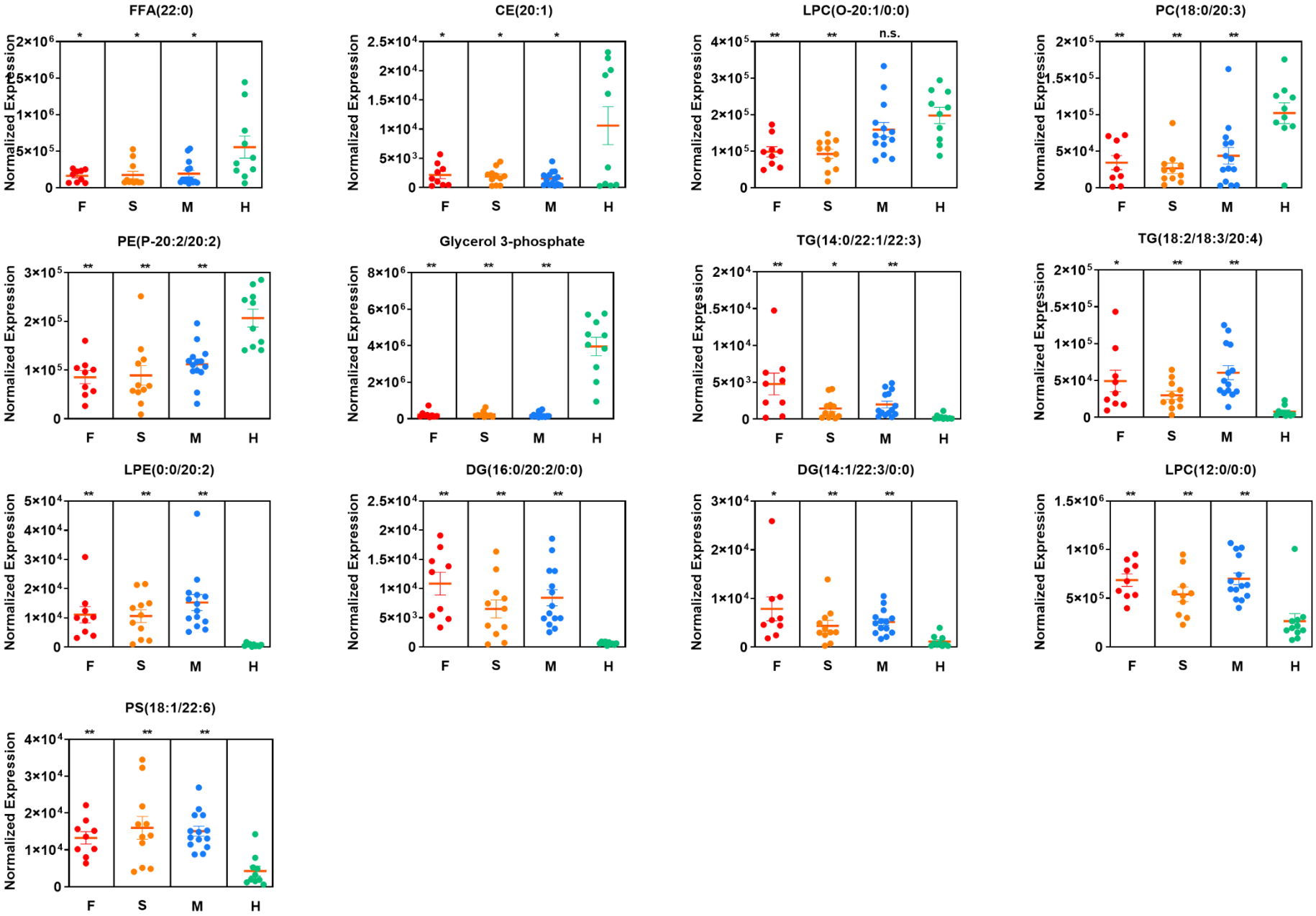
FFA(22:0)
CE(20:1)
LPC(O-20:1/0:0)
PC(18:0/20:3)
PE(P-20:2/20:2)
Glycerol 3-phosphate
TG(14:0/22:1/22:3)
TG(18:2/18:3/20:4)
LPE(0:0/20:2)
DG(16:0/20:2/0:0)
DG(14:1/22:3/0:0)
LPC(12:0/0:0)
PS(18:1/22:6)
Normalized Expression
F
S
M
H
n.s.

Supplementary Data

Supplementary methods and materials

Supplementary Figure S1-S4

Supplementary Table S1-S13

Methods and Materials

Ethics and Human Subjects

All work performed in this study was approved by the Wuhan Jinyintan Hospital Ethics Committee and written informed consent was obtained from patients. Diagnosis of SARS-CoV-2 infection was based on the New Coronavirus Pneumonia Prevention and Control Program (6th edition) published by the National Health Commission of China. Healthy subjects were recruited from healthcare workers and laboratory workers at Wuhan Jinyintan Hospital and Wuhan Institute of Virology, CAS, none of whom had previously experienced SARS-CoV-2 infection.

Patient Samples

SARS-CoV-2-positive patients were enrolled in the study after diagnosis. Blood sample (≤3mL) from fatal COVID-19 patients were collected over the course of their disease at intervals of 3-5 days. Blood sample (≤3mL) from the patients with severe and mild symptoms were collected at the time when the disease were most serious (3-7 days after hospitalization) and the time before discharge. Single samples were collected from healthy patients recruited from healthcare workers and laboratory workers at Wuhan Jinyintan Hospital and Wuhan Institute of Virology. All samples were collected using potassium-EDTA blood collection tubes. All samples used in this study are described in Table S1. All the blood samples were treated according to the biocontainment procedures of the processing of SARS-CoV-2-positive sample.

Methods for extraction of hydrophilic and hydrophobic compounds

To analysis hydrophilic compounds, sample was thawed on ice, 3 volumes of ice-cold methanol was added to 1 volume of plasma/serum, whirled the mixture for 3 min and centrifuge it with 12,000 g at 4℃ for 10 min. Then the supernatant was centrifuged at 12,000 g at 4℃ for 5 min, and then collected the supernatant and subjected them to LC-MS/MS analysis.

To analysis hydrophobic compounds, sample was thawed on ice, whirl around 10 s, and then centrifuge it with 3000 g at 4℃ for 5 min. Take 50 μL of one sample and homogenized it with 1mL mixture (include methanol，MTBE and internal standard mixture). Whirled the mixture for 2 min. Then added 500 μL of water and whirled the mixture for 1 min, and centrifuged it with 12,000 g at 4℃ for 10 min. Extracted 500 μL supernatant and concentrated it. Dissolved powder with 100 μL mobile phase B and subjected to LC-MS/MS analysis.

UPLC conditions of hydrophilic and hydrophobic compounds

The sample extracts of hydrophilic compounds were analyzed using an LC-ESI-MS/MS system (UPLC, Shim-pack UFLC SHIMADZU CBM A system, https://www.shimadzu.com/; MS, QTRAP® System, https://sciex.com/). The analytical conditions were as follows, UPLC: column, Waters ACQUITY UPLC HSS T3 C18 (1.8 μm, 2.1 mm×100 mm); column temperature, 40℃; flow rate, 0.4 mL/min; injection volume, 2μL; solvent system,water (0.1% formic acid): acetonitrile (0.1% formic acid); gradient program, 95:5 V/V at 0 min, 10:90 V/V at 11.0 min,10:90 V/V at 12.0 min, 95:5 V/V at 12.1.

The sample extracts of hydrophobic compounds were analyzed using an LC-ESI-MS/MS system (UPLC, Shim-pack UFLC SHIMADZU CBM A system, https://www.shimadzu.com/; MS, QTRAP® System, https://sciex.com/). The analytical conditions were as follows, UPLC: column, Thermo C30 (2.6μm, 2.1 mm×100 mm); solvent system, A: acetonitrile/water (60/40V,0.04% acetic acid, 5 mmol/L ammonium formate), B: acetonitrile/isopropanol (10/90 V, 0.04% acetic acid, 5 mmol/L ammonium formate); gradient program, A/B（80:20 V/V）at 0 min, 50:50 V/V at 3.0 min, 35:65 V/V at 5 min, 25:75 V/V at 9 min, 10:90 V/V at 15.5 min; flow

rate, 0.35 ml/min; temperature, 45℃; injection volume: 2μL. The effluent was alternatively connected to an ESI-triple quadrupole-linear ion trap (QTRAP)-MS.

ESI-Q TRAP-MS/MS of hydrophilic and hydrophobic compounds

LIT and triple quadrupole (QQQ) scans were acquired on a triple quadrupole-linear ion trap mass spectrometer (QTRAP), QTRAP® LC-MS/MS System, equipped with an ESI Turbo Ion-Spray interface, operating in positive and negative ion mode and controlled by Analyst 1.6.3 software (Sciex). The ESI source operation parameters were as follows: ion source, turbo spray; source temperature 550 ℃; ion spray voltage (IS) 5500 V; ion source gas I (GSI), gas II (GSII), curtain gas (CUR) were set at 55, 60, and 25 psi, respectively; the collision gas (CAD) was medium. Instrument tuning and mass calibration were performed with 10 and 100 μmol/L polypropylene glycol solutions in QQQ and LIT modes, respectively. QQQ scans were acquired as MRM experiments with collision gas (nitrogen) set to 5 psi. DP and CE for individual MRM transitions was done with further DP and CE optimization. A specific set of MRM transitions were monitored for each period according to the metabolites eluted within this period.

Plasma mentalities and lipids data analysis

The mass spectrum data were processed by Software Analyst 1.6.3. The repeatability of metabolite extraction and detection can be judged by total ion current (TIC) and multi peak MRM. Based on MWDB (metadata database) and other databases, qualitative analysis of information and secondary general data was carried out according to retention time (RT) and letter ion. Metabolite structure analysis referred to some existing mass spectrometry public databases, mainly including massbank (http://www.massbank.jp/), knapsack (http://kanaya.naist.jp/knapsack/), HMDB (http://www.hmdb.ca/), moto dB (http://www.ab.wur.nl/moto/) and metlin (http://metlin.scripps.edu/index.php).

Metabolite quantification was accomplished by using multiple reaction monitoring (MRM) of triple quadrupole mass spectrometry. Opened the mass

spectrum file under the sample machine with multiquant software to integrated and calibrated the chromatographic peaks. The peak area of each chromatographic peak represented the relative content of the corresponding substance. Finally, exported all the integral data of chromatographic peak area to save, and used the self-built software package to remove the positive and negative ions of metabolites.

To maximize identification of differences in metabolic profiles between groups, the orthogonal projection to latent structure discriminant analysis (OPLS-DA) model was applied using the MetaboAnalyst R package. The OPLS-DA model was evaluated with the relevant R2 and Q2. And we used the permutation to assess the risk that the current OPLS-DA model is spurious.

Pathway Enrichment

We used the Kyoto Encyclopedia of Genes and Genomes (KEGG) database (http://www. genome.Jp/kegg/) to analyze the KEGG pathway enrichment to find highly enriched metabolic signal transduction pathways in differential metabolites or lipids. The p-value <0.05 was considered significantly changing pathways and was used for subsequent analysis.

Statistically Processed Datasets

Plasma metabolomics and lipidomics datasets (including fold-change and *P*-values for various group comparisons) are provided in Table S4-S5 and S8-S9. Plasma metabolomics pathway enrichment are provided in Table S6-S7. Plasma lipidomic pathway enrichment are provided in Table S10-S11.

Raw Data

All raw LC-MS/MS data has been deposited to the iProX under the accession number: PXD018307.

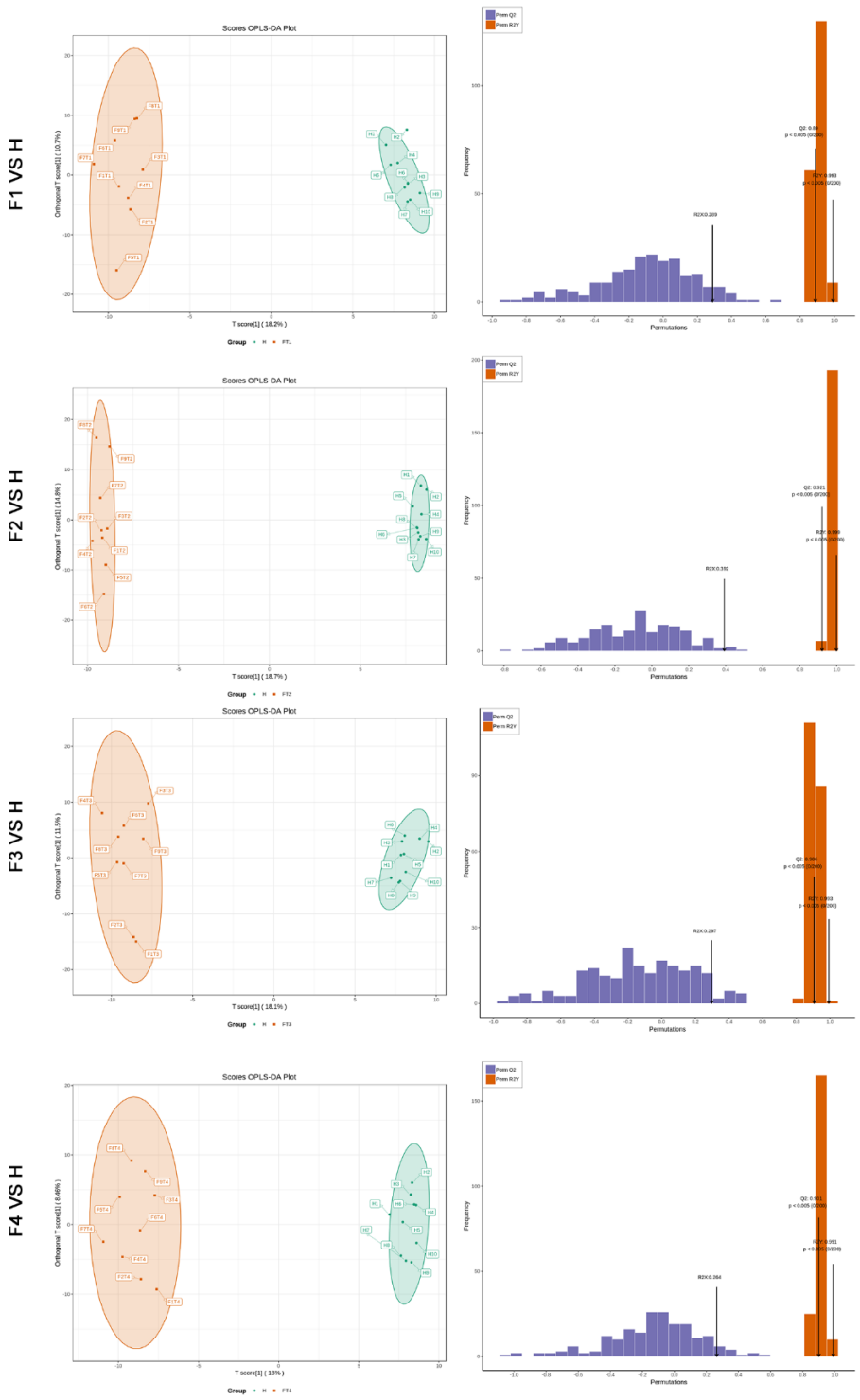

Figure S1. The orthogonal projection to latent structure discriminant analysis (OPLS-DA) showed the best possible discrimination of metabolites between fatal COVID-19 patients and healthy people as indicated. The x-axis represents the prediction component that shows differences between groups, and the y-axis represents the orthogonal component differences within the group. R2 represents goodness of fit, Q2 represents goodness of prediction, and P value shows the significance level of the model (x-axis = predictive components, y-axis = orthogonal component).

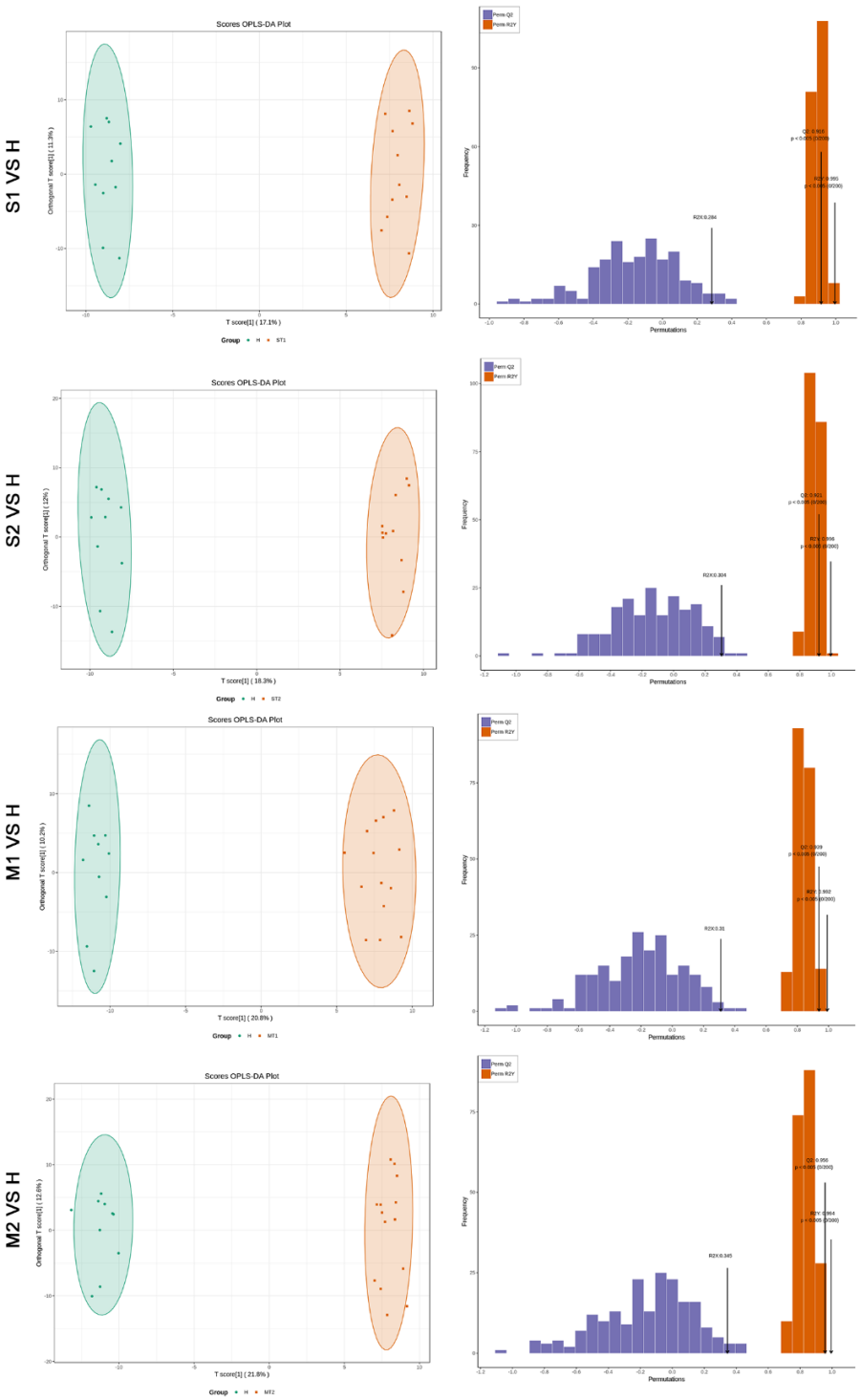

Figure S2. The OPLS-DA showed the best possible discrimination of metabolites between severe or mild COVID-19 patients and healthy people as indicated. The x-axis represents the prediction component that shows differences between groups, and the y-axis represents the orthogonal component differences within the group. R2 represents goodness of fit, Q2 represents goodness of prediction, and P value shows the significance level of the model (x-axis = predictive components, y-axis = orthogonal component).

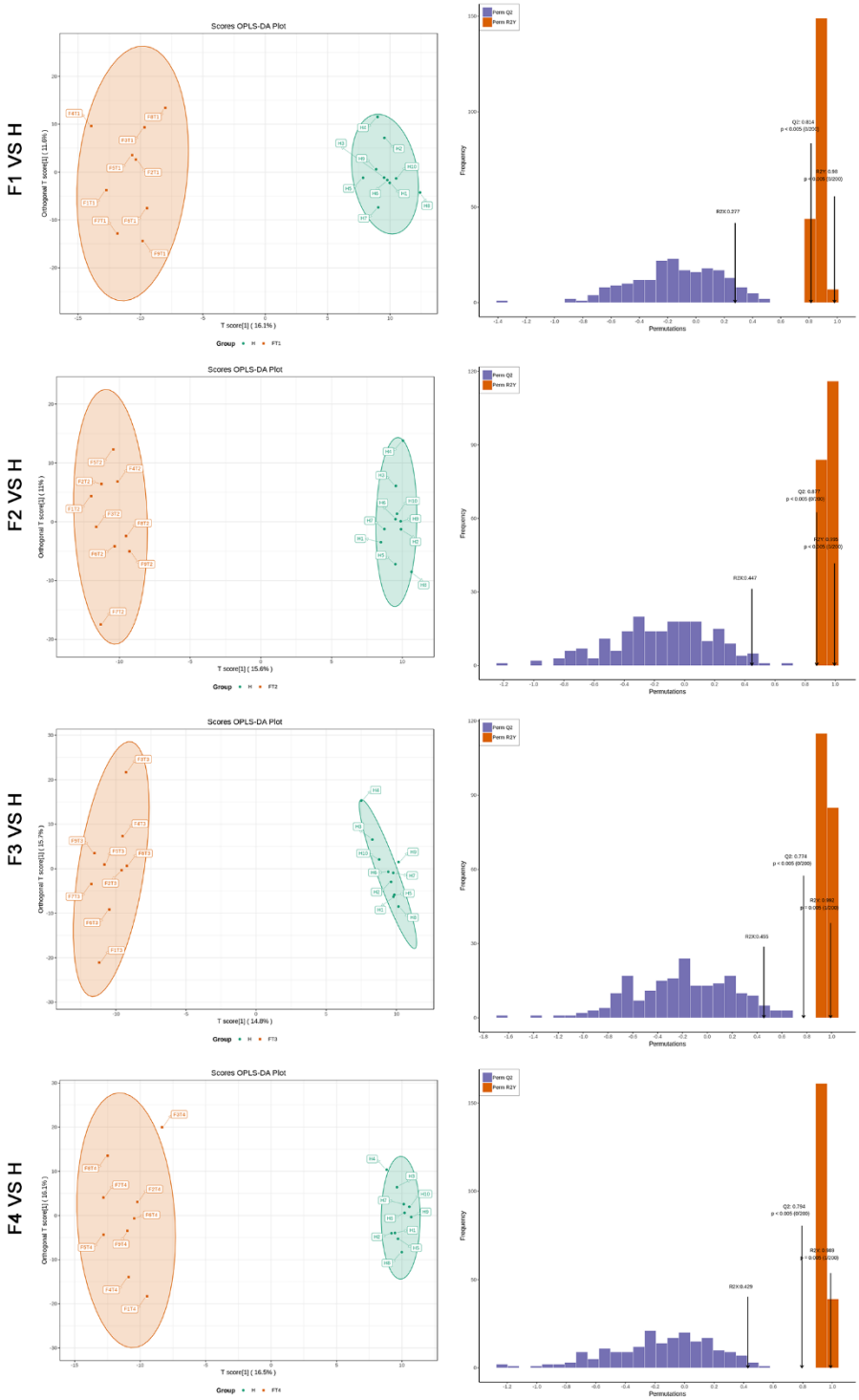

Figure S3. The OPLS-DA showed the best possible discrimination of lipids between fatal COVID-19 patients and healthy people as indicated. The x-axis represents the prediction component that shows differences between groups, and the y-axis represents the orthogonal component differences within the group. R2 represents goodness of fit, Q2 represents goodness of prediction, and P value shows the significance level of the model (x-axis = predictive components, y-axis = orthogonal component).

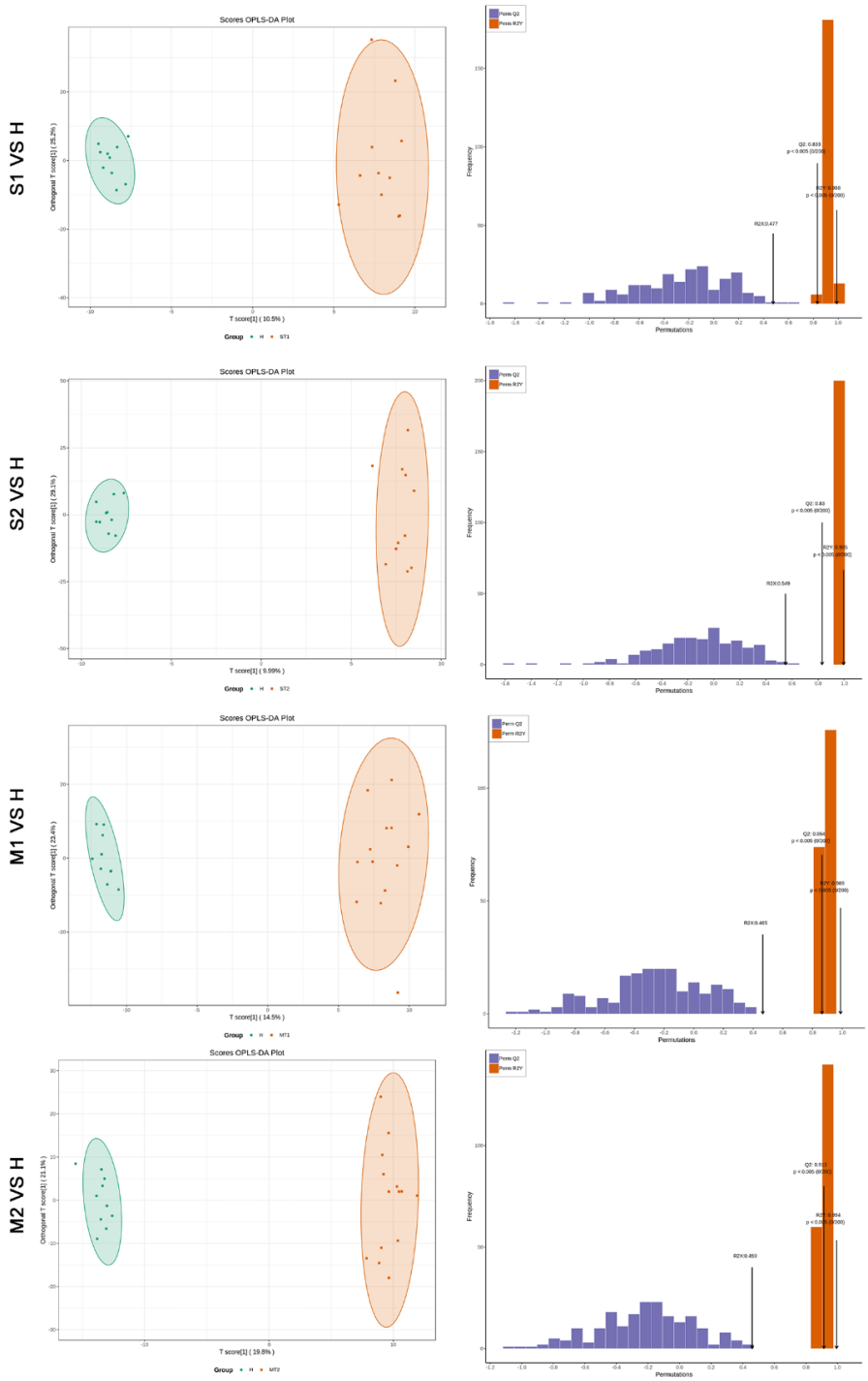

Figure S4. The OPLS-DA showed the best possible discrimination of lipids between severe or mild COVID-19 patients and healthy people as indicated. The x-axis represents the prediction component that shows differences between groups, and the y-axis represents the orthogonal component differences within the group. R2 represents goodness of fit, Q2 represents goodness of prediction, and P value shows the significance level of the model (x-axis = predictive components, y-axis = orthogonal component).

Table S1. Study design and patients

	Fatal (F)				Severe (S)		Mild (M)		Healthy (H)
	T1	**T2**	**T3**	**T4**	**T1**	**T2**	**T1**	**T2**	**H**
Onset to hospitalization	1. 8	5.1	10.1	14.8	5. 4	15.4	5.2	13	NA
Days (SD)	(0.4)	(0.3)	(0.3)	(1.2)	(3.1)	(4.8)	(0.6)	(0)	NA
Sex									
Female		5			8		9		5
Male		4			3		5		5
Age		64.6			57.4		45.9		48.7
Mean (SD)		(8.5)			(12.5)		(11.8)		(9.6)
Patients		9			11		14		10
Sample number		(36)			(22)		(28)		(10)

Table S2. Overview of total changed metaboites

Total metaboites (431)	Metabolites（p <0.05）	Up-regulated	wn-regula	ax (Log_2F	Min (Log_2FC)
F1 vs. H	87	4	83	2.17	-5.19
F2 vs. H	164	19	145	1.95	-8.98
F3 vs. H	172	45	127	2.6	-8.66
F4 vs. H	162	51	111	2.87	-6.67
S1 vs. H	142	23	119	1.73	-6.79
S2 vs. H	154	24	130	1.68	-7.03
M1 vs. H	190	28	162	1.36	-5.58
M2 vs. H	203	49	154	1.97	-8.29

Table S2. Overview of total changed lipids

Total lipid (698)	Lipids (p <0.05)	Up-regulated	Down-regulated	Max (Log_2FC)	Min (Log_2FC)
F1 vs. H	255	111	144	4.54	-3.02
F2 vs. H	203	134	69	4.2	-3.6
F3 vs. H	221	135	86	4.23	-3.6
F4 vs. H	248	152	96	2.29	-4.1
S1 vs. H	157	57	100	5.37	-4.08
S2 vs. H	158	104	54	4.76	-3.78
M1 vs. H	120	82	38	4.44	-4.23
M2 vs. H	127	93	34	5.61	-3.47

Table S4. Metabolomics data of F vs H

		Log_2 FC				*P* value			
Compounds	Class	F1/H	F2/H	F3/H	F4/H	F1/H-P	F2/H-P	F3/H-P	F4/H-P
N-Acetylmethionine	Amino Acid metabolomics	0.415995	0.384181	-0.5209	1.472419	0.287154	0.343777	0.17238	0.024861
5-Oxoproline	Amino Acid metabolomics	-0.44792	-0.37169	-0.60266	-1.00112	0.004439	0.010616	0.001122	3.28E-05
H-Homoarg-Oh	Amino Acid metabolomics	-0.28014	-0.58468	-0.56313	-1.05239	0.110157	0.007977	0.054885	0.00112
L-Dopa	Amino Acid metabolomics	-2.44123	-0.23573	0.000169	-1.05478	0.00192	0.382964	0.499918	0.032538
L-Cysteine	Amino Acid metabolomics	-1.0712	-1.43904	-0.97253	-1.06373	0.000873	0.000142	0.005008	0.000827
3-Hydroxykynurenine	Amino Acid metabolomics	-1.17707	-0.57529	-1.12227	-1.25096	0.045701	0.163655	0.053317	0.043201
N-Alpha-Acetyl-L-Asparagine	Amino Acid metabolomics	-2.10692	-1.96952	-1.86819	-1.28968	0.001101	0.001375	0.002018	0.021265
Cis-Aconitic Acid	Amino Acid metabolomics	-1.1208	-0.85778	-0.87544	-1.44704	0.004077	0.015425	0.011871	0.001304
N-Amidino-L-Aspartate	Amino Acid metabolomics	-2.26063	-2.01719	-2.62917	-1.79353	0.021058	0.026302	0.016547	0.031758
N-Acetylneuraminic Acid	Amino Acid metabolomics	-1.66003	-1.93639	-2.43783	-1.86305	0.00357	0.002239	0.001227	0.002507
L-Alanyl-L-Lysine	Amino Acid metabolomics	-1.14071	-1.42885	-1.5164	-1.87558	0.074097	0.044202	0.039995	0.026026
N-Acetyl-L-Leucine	Amino Acid metabolomics	-1.76235	-2.30942	-1.7829	-1.94925	0.000155	3.59E-05	0.000107	0.000104
L-Cystine	Amino Acid metabolomics	-0.80689	-0.9762	-1.7953	-2.4699	0.138564	0.107133	0.035476	0.020686
(5-L-Glutamyl)-L-Amino Acid	Amino Acid metabolomics	-1.71512	-2.25523	-2.26179	-2.71761	0.06058	0.041274	0.041316	0.032937
Sarcosine	Amino Acid metabolomics	-3.61293	-1.1137	-1.64117	-3.05146	5.92E-05	0.021791	0.002939	7.78E-05
L-Aspartic Acid	Amino Acid metabolomics	-2.91658	-3.2912	-2.60625	-3.46617	0.001052	0.000866	0.001328	0.000805
Citramalic Acid	Amino Acid metabolomics	-3.54815	-3.18379	-3.32691	-3.71531	0.027899	0.0308	0.029504	0.026891
N-Glycyl-L-Leucine	Amino Acid metabolomics	-3.00807	-3.06715	-3.77884	-3.72516	0.037444	0.0368	0.03074	0.031086
Nα-Acetyl-L-Arginine	Amino Acid metabolomics	-3.29207	-3.32587	-4.00324	-4.04416	0.0014	0.001354	0.001101	0.001088
L-Malic Acid	Amino Acid metabolomics	-3.20684	-3.56382	-3.22737	-5.17882	0.011408	0.010077	0.011437	0.00755
Uridine triphosphate (UTP)	Nucleotide metabolomics	-2.35267	-1.10822	0.698174	2.870307	0.008814	0.066465	0.229133	0.038229
deoxyguanosine 5'-monophosph	Nucleotide metabolomics	1.506003	0.465777	0.74978	1.643068	0.043023	0.174352	0.060583	0.022884
Hypoxanthine	Nucleotide metabolomics	-0.03789	0.596264	0.444553	1.519397	0.472157	0.012469	0.085358	0.005911
3'-Aenylic Acid	Nucleotide metabolomics	1.392182	0.599545	0.442721	1.267303	0.07564	0.156508	0.169316	0.038121
5-Methyluridine	Nucleotide metabolomics	0.772244	0.763794	1.568552	1.231203	0.015445	0.032614	0.001086	0.000223
5-Methylcytosine	Nucleotide metabolomics	-0.5228	-0.52529	-0.43656	-1.24787	0.036938	0.145603	0.0964	0.001179
Guanosine Monophosphate	Nucleotide metabolomics	-1.01085	-2.37581	-1.82318	-1.70981	0.010877	0.000136	0.00038	0.001009
Dihydrouracil	Nucleotide metabolomics	-2.14036	-1.3746	-2.35803	-1.92621	0.000482	0.004177	0.000351	0.000658
B-Pseudouridine	Nucleotide metabolomics	-2.8951	-2.81071	-2.23919	-2.51716	0.026622	0.027609	0.037165	0.031548
N1-Acetylspermine	Organic Acid And Its Derivatives	1.018201	1.116511	1.75383	1.935243	0.086981	0.094542	0.038839	0.043907
N-lactoyl-phenylalanine	Organic Acid And Its Derivatives	0.284114	0.903021	1.471939	1.557709	0.180991	0.028992	0.018665	0.001141
Mandelic Acid	Organic Acid And Its Derivatives	0.097444	1.720012	1.646997	1.321685	0.433151	0.152779	0.004443	0.028818
3-Hydroxy-3-Methyl Butyric Ac	Organic Acid And Its Derivatives	0.577804	0.939791	1.253056	1.166969	0.066867	0.058533	0.007174	0.000344
Phenyllactate (Pla)	Organic Acid And Its Derivatives	-0.06936	0.558789	1.136635	1.141882	0.377323	0.07222	0.014987	0.000165
4-Hydroxy-2-Oxoglutaric Acid	Organic Acid And Its Derivatives	-0.68396	-0.91053	-1.11942	-1.30552	0.150699	0.072493	0.047183	0.025974
Indoxylsulfuric acid	Organic Acid And Its Derivatives	-0.92087	-1.45775	-0.98194	-1.48366	0.09223	0.037637	0.140108	0.008873
Dl-2-Aminooctanoic Acid	Organic Acid And Its Derivatives	-1.2446	-1.25563	-1.28252	-1.49751	0.013493	0.013603	0.012673	0.007329
2-Aminoethanesulfinic Acid	Organic Acid And Its Derivatives	-1.28001	-1.49647	-1.14454	-1.75835	0.018538	0.011769	0.024911	0.007733
L-Methionine Sulfoximine	Organic Acid And Its Derivatives	-2.3071	-2.50929	-2.36262	-2.66533	0.029152	0.025944	0.02827	0.023882
2-Hydroxyisocaproic Acid	Organic Acid And Its Derivatives	-3.79046	-3.166	-3.02956	-2.80525	0.033511	0.038663	0.040249	0.043468
O-Acetyl-L-serine	Organic Acid And Its Derivatives	-3.2341	-3.12477	-4.0451	-2.95325	0.000253	0.000249	0.000186	0.000296
Phenylpyruvic Acid	Organic Acid And Its Derivatives	-2.73737	-2.69577	-3.52819	-3.24768	0.04059	0.041016	0.031297	0.033791
Ergothioneine	Organic Acid And Its Derivatives	-3.44893	-4.15286	-3.89269	-3.51253	0.025414	0.021958	0.022974	0.02504
Carbamoyl phosphate	Organic Acid And Its Derivatives	-1.52663	-2.04206	-2.66607	-3.66684	0.005934	0.003345	0.000859	0.000498
Isonicotinic acid	Organic Acid And Its Derivatives	-3.87955	-5.64861	-4.95553	-4.63743	0.015038	0.012061	0.012761	0.013237
Allantoin	Organic Acid And Its Derivatives	-4.39518	-4.18629	-4.03702	-4.96958	0.000222	0.000232	0.00024	0.000205
Acetaminophen Glucuronide	Carbohydrate metabolomics	-0.23092	0.19609	1.149391	1.676664	0.309097	0.327722	0.0642	0.039242
L-Erythrulose	Carbohydrate metabolomics	-0.07649	0.154722	0.988749	1.020589	0.395382	0.3952	0.021339	0.002354
Lactose	Carbohydrate metabolomics	-2.23636	-1.62366	-2.31481	-1.39533	0.007651	0.015876	0.007172	0.023111
D-Glucoronic Acid	Carbohydrate metabolomics	-2.44351	-1.44762	-1.31233	-1.50387	0.010938	0.038143	0.040094	0.029705
Gluconic Acid	Carbohydrate metabolomics	-2.016	-1.88748	-1.60319	-1.53276	0.011158	0.012942	0.020542	0.020747
L-Gulonic-Γ-Lactone	Carbohydrate metabolomics	-1.39377	-1.5114	-1.55071	-1.7001	0.023793	0.019213	0.01821	0.014752
D-Xylulose 5-phosphate	Carbohydrate metabolomics	-1.11063	-1.93107	-1.509	-1.81924	0.000586	9.41E-07	1.36E-06	9.22E-07
L-Rhamnose	Carbohydrate metabolomics	-0.40252	-0.61925	-1.43985	-2.01665	0.273561	0.191244	0.024744	0.008734
D-Mannitol	Carbohydrate metabolomics	-4.20079	-4.48232	-3.57985	-2.11633	0.001542	0.001459	0.001852	0.010299
L-Fucose	Carbohydrate metabolomics	-0.63058	-1.15542	-1.92933	-3.01374	0.195917	0.072636	0.017853	0.007786
1,5-Anhydro-D-Glucitol	Carbohydrate metabolomics	-1.52616	-1.56935	-2.25716	-3.08623	0.042433	0.040865	0.020769	0.012689
Scyllo inositol	Alcohol	-0.0501	0.079144	1.155304	1.70685	0.467608	0.443926	0.043812	0.036731
2-Methyl-5-nitroimidazole-1-eth	Alcohol	2.16995	1.669196	1.664315	1.410794	0.035451	0.008609	0.026476	0.01455
Norambreinolide	Lactone	-0.7142	-0.74474	-0.70192	-1.16607	0.025494	0.036359	0.031972	0.002874
1-Aminopropan-2-ol	Alcohol	-1.49129	-1.78829	-1.29994	-2.15193	0.007199	0.004342	0.032604	0.0007
Isoxanthopterin	Pteridines and derivatives	-2.53133	-3.01891	-2.60004	-2.67619	0.028668	0.022972	0.02753	0.026513
Cyclohexylamine	Amines	-0.55378	-2.93483	-2.7271	-2.74338	0.225179	0.000345	0.00041	0.000398
Putrescine	Polyamine	-2.84497	-2.65947	-2.7034	-2.85256	4.09E-08	4.49E-08	4.08E-08	5.05E-08
Serotonin	Indole And Its Derivatives	-2.82246	-3.88391	-3.8003	-2.87434	0.028876	0.020617	0.020843	0.028125
Neopterin	Pteridines and derivatives	-2.78751	-3.03666	-2.81618	-3.22401	0.00018	0.000175	0.000165	0.000154
Indole-3-acetamide	Indole And Its Derivatives	-3.73138	-3.92199	-3.10611	-3.51775	0.005064	0.004806	0.006411	0.005419
2-Picoline	Pyridine And Pyridine Derivatives	-2.36222	-2.82098	-3.26161	-3.57434	0.027215	0.020039	0.016677	0.015152
Sn-Glycero-3-Phosphocholine	Cholines	-4.97371	-5.33267	-5.30757	-4.82431	0.036745	0.03588	0.035936	0.037184
δ-Valerolactam	Pyridine And Pyridine Derivatives	-0.63915	-4.15741	-4.23946	-5.3341	0.223001	0.000547	0.000547	0.000461
3-Indolepropionic Acid	Indole And Its Derivatives	-4.92956	-7.22645	-8.66206	-6.67477	0.000324	0.000282	0.000275	0.000288
Estrone	Hormones	-0.14546	0.019546	0.857123	1.206206	0.356343	0.484587	0.105574	0.045538
L-Thyroxine	Hormones	-0.18812	-0.40077	-0.64946	-1.007	0.027729	0.003561	1.99E-05	1.64E-05
octadecanedioate (C18)	Hydrocarbon derivative	-0.11808	0.393535	1.354421	-1.10991	0.403896	0.297186	0.175989	0.012956
3,3',5-Triiodo-L-Thyronine	Hormones	-1.27934	-1.67931	-1.84553	-1.49267	9.33E-08	3.32E-09	1.67E-10	1.31E-06
Orotic Acid	CoOthersEnzyme Factor & vitamin	-1.61001	-1.35304	-1.62917	-1.90883	0.011821	0.018127	0.011414	0.007366
Glycyrrhetinic acid	Terpenoid	-1.34991	0.243521	-1.61381	-2.20727	0.088821	0.421176	0.070649	0.044583
1,2-Dichloroethane	Hydrocarbon derivative	-5.18782	-5.22336	-5.24624	-5.29574	0.043742	0.04365	0.043591	0.043469

Table S5. Metabolomics data of S vs H and M vs H

		Log_2 FC				*P* value			
Compounds	Class	ST1/H	ST2/H	MT1/H	MT2/H	ST1/H-P	ST2/H-P	MT1/H-P	MT2/H-P
Phe-Phe	Amino Acid metabolomics	-1.05907	-1.22584	-1.68646	-1.11816	0.004679	0.001421	0.000194	0.001817
Succinic Acid	Amino Acid metabolomics	-1.26589	-1.31493	-1.30385	-1.15697	3.39E-05	0.00033	1.08E-05	3.47E-05
L-Cystathionine	Amino Acid metabolomics	-1.75346	-2.40893	-2.4026	-2.43225	0.001732	0.000694	0.000658	0.000684
L-Dopa	Amino Acid metabolomics	-2.29428	-2.44311	-2.31547	-2.39848	0.00221	0.001902	0.002148	0.001995
3-Hydroxykynurenine	Amino Acid metabolomics	-1.79187	-1.81586	-1.22318	-1.5395	0.019565	0.018852	0.044288	0.027321
N-Alpha-Acetyl-L-Asparagine	Amino Acid metabolomics	-2.55805	-2.84708	-3.13325	-2.90126	0.000641	0.00054	0.000456	0.000497
N-Amidino-L-Aspartate	Amino Acid metabolomics	-2.4207	-2.44172	-2.93977	-1.89163	0.018657	0.018383	0.014024	0.028521
N-Acetylneuraminic Acid	Amino Acid metabolomics	-2.39427	-2.81504	-2.41294	-2.36857	0.001315	0.000915	0.001284	0.001342
L-Alanyl-L-Lysine	Amino Acid metabolomics	-2.1086	-2.80481	-3.13307	-2.75344	0.021387	0.013464	0.011621	0.013827
N-Acetyl-L-Leucine	Amino Acid metabolomics	-2.84734	-3.00383	-2.74394	-3.22376	3.05E-05	2.82E-05	3.25E-05	2.69E-05
L-Cystine	Amino Acid metabolomics	-1.45739	-1.2129	-1.54213	-1.09267	0.049181	0.068311	0.044405	0.08065
Sarcosine	Amino Acid metabolomics	-3.71742	-3.61035	-3.68509	-3.08786	5.74E-05	6.02E-05	5.84E-05	6.11E-05
L-Aspartic Acid	Amino Acid metabolomics	-5.09458	-4.99467	-4.64915	-4.92532	0.000538	0.000545	0.000577	0.00055
Citramalic Acid	Amino Acid metabolomics	-4.1258	-4.24022	-3.82169	-3.73401	0.024971	0.024544	0.026321	0.02678
N-Glycyl-L-Leucine	Amino Acid metabolomics	-3.5852	-3.4577	-3.09782	-2.14804	0.031968	0.032888	0.036245	0.05473
Nα-Acetyl-L-Arginine	Amino Acid metabolomics	-4.14903	-3.92033	-3.95763	-3.96719	0.001059	0.001127	0.001115	0.001113
L-Malic Acid	Amino Acid metabolomics	-4.79583	-4.29492	-4.43537	-4.21497	0.007876	0.008492	0.008291	0.008613
5'-Deoxy-5'-(Methylthio) Adeno	Nucleotide metabolomics	-4.33756	-4.51862	-5.26895	-5.09976	6.49E-05	6.39E-05	5.61E-05	5.75E-05
Uridine triphosphate (UTP)	Nucleotide metabolomics	-2.04085	-1.57538	-2.17407	-1.99955	0.01341	0.029289	0.010212	0.012556
Inosine	Nucleotide metabolomics	-2.15734	-1.86936	-2.55038	-2.57257	0.030767	0.03871	0.024134	0.023819
Dihydrouracil	Nucleotide metabolomics	-1.91661	-0.85149	-1.7107	-1.80431	0.000679	0.080392	0.001001	0.000855
B-Pseudouridine	Nucleotide metabolomics	-2.87588	-2.7439	-3.10337	-2.96866	0.026856	0.028403	0.02465	0.025864
(3-Methoxy-4-hydroxyphenyl)et	Organic Acid And Its Derivatives	-1.18864	-1.22015	-1.69221	-1.26818	0.000859	0.000572	3.03E-05	0.002261
3-Methoxy-4-Hydroxyphenyleth	Organic Acid And Its Derivatives	-3.18165	-3.04456	-3.22145	-1.01645	2.63E-08	7.5E-08	2.68E-09	0.052916
Chlorogenic Acid	Organic Acid And Its Derivatives	-2.45078	-0.33704	-2.15271	-1.80269	0.033452	0.375682	0.040191	0.051511
N'-Formylkynurenine	Organic Acid And Its Derivatives	-2.15872	-2.34291	-3.20625	-1.60316	0.004476	0.00407	0.001892	0.014664
4-Hydroxy-2-Oxoglutaric Acid	Organic Acid And Its Derivatives	-1.72477	-1.87049	-2.1295	-1.98913	0.013538	0.011735	0.008232	0.009978
2-Aminoethanesulfinic Acid	Organic Acid And Its Derivatives	-2.01329	-1.95467	-1.74297	-1.40494	0.005424	0.00586	0.007665	0.013454
L-Methionine Sulfoximine	Organic Acid And Its Derivatives	-2.99569	-3.04154	-3.20485	-3.25766	0.020644	0.020287	0.019134	0.018808
2-Hydroxyisocaproic Acid	Organic Acid And Its Derivatives	-3.65183	-3.68696	-3.65882	-3.90716	0.034403	0.034179	0.034356	0.032817
O-Acetyl-L-serine	Organic Acid And Its Derivatives	-4.64275	-4.7768	-4.43183	-4.37769	0.000173	0.000171	0.000183	0.000184
Phenylpyruvic Acid	Organic Acid And Its Derivatives	-4.88666	-4.97877	-5.57542	-6.02016	0.025569	0.025367	0.02435	0.02384
Ergothioneine	Organic Acid And Its Derivatives	-4.14382	-3.93661	-4.47123	-4.52811	0.021969	0.022773	0.020962	0.020814
Carbamoyl phosphate	Organic Acid And Its Derivatives	-2.95773	-3.14693	-2.65585	-1.92833	0.000721	0.000652	0.000916	0.002048
Isonicotinic acid	Organic Acid And Its Derivatives	-4.46446	-4.67356	-4.85806	-3.88969	0.013544	0.01317	0.012883	0.015022
Allantoin	Organic Acid And Its Derivatives	-5.26089	-5.36381	-5.19391	-4.53726	0.000198	0.000195	0.000199	0.000221
Xylose	Carbohydrate metabolomics	-1.05358	-0.93967	-1.90435	-1.59997	0.049472	0.044314	0.006956	0.010725
Lactose	Carbohydrate metabolomics	-2.33865	-1.59596	-2.22555	-1.74122	0.006982	0.017006	0.007998	0.017256
D-Glucoronic Acid	Carbohydrate metabolomics	-2.6799	-2.50784	-3.24887	-2.81335	0.00936	0.010459	0.007056	0.008659
Gluconic Acid	Carbohydrate metabolomics	-2.8526	-1.95587	-2.18514	-2.15168	0.005707	0.012113	0.00941	0.010061
L-Gulonic-Γ-Lactone	Carbohydrate metabolomics	-1.59401	-1.74175	-1.67023	-1.71872	0.016927	0.013882	0.01525	0.014306
D-Xylulose 5-phosphate	Carbohydrate metabolomics	-1.44464	-1.0516	-1.42367	-0.96677	2.33E-06	4.05E-05	2.63E-06	2.61E-05
L-Rhamnose	Carbohydrate metabolomics	-2.9302	-3.48255	-2.80808	-4.14459	0.004048	0.003128	0.004362	0.002567
D-Mannitol	Carbohydrate metabolomics	-5.40154	-4.78257	-5.54389	-5.13857	0.001281	0.001388	0.001264	0.00132
L-Fucose	Carbohydrate metabolomics	-3.59767	-4.05648	-3.53633	-5.07376	0.006158	0.005436	0.006285	0.004606
1,5-Anhydro-D-Glucitol	Carbohydrate metabolomics	-3.45421	-3.12839	-3.06714	-5.04605	0.011139	0.012634	0.012798	0.00815
2-Methyl-5-nitroimidazole-1-eth	Alcohol	1.733934	1.67861	1.360682	1.968403	0.004635	0.001952	4.49E-05	4.68E-06
Pulegone	Ketones	-5.30641	-5.30682	-4.58341	-4.92088	0.01725	0.017249	0.018487	0.017824
4-Pyridoxic Acid	Pyridine And Pyridine Derivatives	-1.59548	-1.56911	-1.34551	-1.49721	0.000156	0.000189	0.000317	0.000165
Methyl Indole-3-Acetate	Indole And Its Derivatives	-1.92096	-1.05716	-2.07051	-1.14229	0.001359	0.011818	0.001121	0.007455
Dopamine	Polyamine	-1.42453	-1.50218	-1.72467	-1.53734	0.000826	0.000679	0.000425	0.000638
Isoxanthopterin	Pteridines and derivatives	-2.08614	-2.46213	-3.61472	-2.214	0.040712	0.029956	0.019093	0.035739
Putrescine	Polyamine	-4.27095	-4.24836	-4.16225	-4.25549	2.18E-07	2.18E-07	2.1E-07	2.03E-07
Serotonin	Indole And Its Derivatives	-4.0889	-3.67607	-3.0202	-2.17333	0.019699	0.021378	0.025962	0.039003
Neopterin	Pteridines and derivatives	-3.48082	-3.56947	-3.72713	-3.57963	0.000137	0.000131	0.000122	0.000131
Indole-3-acetamide	Indole And Its Derivatives	-3.94544	-4.48007	-4.82494	-4.98633	0.004777	0.00427	0.00405	0.003967
2-Picoline	Pyridine And Pyridine Derivatives	-4.34104	-4.40635	-3.98805	-3.95489	0.012886	0.012757	0.013723	0.013819
Sn-Glycero-3-Phosphocholine	Cholines	-4.4319	-3.90612	-3.98443	-3.41891	0.038588	0.041333	0.040842	0.045214
Dethiobiotin	Others	-2.0931	-2.67871	-2.02839	-2.4911	4.23E-05	6.14E-06	2.22E-05	5.48E-06
Triethylamine	Hydrocarbon derivative	-2.53706	-2.34903	-2.01939	-1.99689	0.0026	0.00308	0.004384	0.004513
Orotic Acid	CoOthersEnzyme Factor & vitamin	-2.09137	-2.18934	-2.27894	-2.42636	0.005898	0.005328	0.004879	0.004277
1,2-Dichloroethane	Hydrocarbon derivative	-5.25168	-5.21395	-5.30243	-5.33581	0.043577	0.043673	0.043453	0.043373

Table S6. KEGG enrichment analysis of DEMs shared by F vs H, S vs H and M vs H

#KEGG n	29	KEGG N	231			
#Pathway	ko ID	Unique cor	compound	Uni all	compound	all
Metabolic p	ko01100	26	202	29	231	MEDN240 C01040+C00169+C00507+C05570+C00355+C06752+C00243+C00429+C00149+C00392+C00166+C00491+C02693+C00295+C00231+C00075+C00979+C01127+C00257+C01019+C00213+C00049+C00134+C02067+C00780+C00519
Cysteine an	ko00270	3	18	29	231	MEDN616 C00979+C00049+C00491
ABC transp	ko02010	5	43	29	231	MEDP127 C00134+C00243+C00049+C00392+C00491
Protein dig	ko04974	3	26	29	231	MEDP127 C00134+C00049+C00491
Glycine, se	ko00260	2	19	29	231	MEDN009 C00049+C00213
Arginine ar	ko00330	2	18	29	231	MEDP404 C00213+C00134
Arginine bi	ko00220	2	12	29	231	MEDN615 C00169+C00049
Alanine, as	ko00250	2	11	29	231	MEDN009 C00049+C00169
Histidine m	ko00340	2	8	29	231	MEDP437 C05570+C00049
beta-Alanin	ko00410	2	9	29	231	MEDN009 C00049+C00429
Pantothena	ko00770	2	10	29	231	MEDN009 C00049+C00429
Carbon me	ko01200	6	18	29	231	MEDN009 C00049+C00149+C00231+C00979+C00257+C00169
2-Oxocarbo	ko01210	2	23	29	231	MEDN339 C00166+C00049
Biosynthesi	ko01230	5	49	29	231	MEDN615 C00169+C00049+C00231+C00979+C00166
Neuroactiv	ko04080	3	13	29	231	MEDN009 C00049+C00075+C00780
Central car	ko05230	2	25	29	231	MEDN009 C00049+C00149
Glyoxylate	ko00630	2	12	29	231	MEDN200 C00149+C01127
Taste transd	ko04742	2	11	29	231	MEDP081 C00780+C00149
Pyrimidine	ko00240	5	21	29	231	MEDN244 C00295+C00169+C02067+C00075+C00429
Pentose ph	ko00030	2	6	29	231	MEDP236 C00257+C00231
Ascorbate a	ko00053	2	6	29	231	MEDN240 C01040+C00231
Fructose ar	ko00051	3	5	29	231	MEDN232 C00507+C01019+C00392
Tryptophar	ko00380	2	17	29	231	MEDP081 C00780+C02693

Table S7. KEGG enrichment analysis of DEMs unique to F vs H

#KEGG	n 13	KEGG	N 231			
#Pathway	ko ID	Unique cor	compound	Uni all	compound	all
Metabolic p	ko01100	13	202	13	231	MEDP036: C02237+C00144+C02376+C01829+C00468+C00262+C03740+C06153+C00362+C01367+C00417+C00097+C02465
Glutathione	ko00480	2	12	13	231	MEDP028: C03740+C00097
Purine met	ko00230	4	16	13	231	MEDN163 C00262+C01367+C00362+C00144
Tyrosine m	ko00350	2	19	13	231	MEDN179 C01829+C02465
Neuroactiv	ko04080	2	13	13	231	MEDN179 C01829+C02465
Thyroid ho	ko04918	2	6	13	231	MEDN179 C01829+C02465
Thyroid ho	ko04919	2	3	13	231	MEDN179 C01829+C02465
Bile secreti	ko04976	2	11	13	231	MEDP184: C02465+C01829
Autoimmu	ko05320	2	2	13	231	MEDN179 C01829+C02465

Table S8. Lipidomic data of F vs H

		Log_2 FC				*P* value			
Compounds	Class	F1/H	F2/H	F3/H	F4/H	F1/H-P	F2/H-P	F3/H-P	F4/H-P
3-Hydroxy-tetradecenoyl- carnit	CAR	0.732891	1.058621	0.936478	1.322227	0.035259	0.006774	0.003624	0.003958
CE(18:0)	CE	-0.65621	-0.78053	-0.9131	-1.32363	0.017791	0.008787	0.003213	0.000636
Cer(d18:0/18:0)	Cer	1.837063	1.945024	1.959347	1.863655	0.000374	0.001599	0.011023	0.002918
DG(16:0/20:2/0:0)	DG	3.156343	3.856241	3.285843	4.154154	0.02941	0.024028	0.01167	0.014896
DG(14:1/22:3/0:0)	DG	1.757707	1.36161	1.832577	2.79635	0.001871	0.000903	0.001274	0.004844
DG(16:0/16:1/0:0)	DG	1.881072	2.126148	1.704713	2.106992	0.005756	0.005341	0.005894	0.000544
DG(16:1/18:3/0:0)	DG	1.941991	1.465783	1.300218	2.034405	0.00183	0.002259	0.001397	0.000398
DG(16:1/20:2/0:0)	DG	1.072046	1.264273	1.538108	1.928656	0.034651	0.017008	0.014229	0.0011
DG(18:2/20:1/0:0)	DG	0.607559	0.974156	0.852753	1.760549	0.165856	0.057757	0.087492	0.009319
DG(18:1/20:5/0:0)	DG	0.5807	0.903268	1.303825	1.638523	0.168058	0.056314	0.039592	0.007025
DG(14:1/22:2/0:0)	DG	0.932721	0.848304	1.141428	1.60097	0.071348	0.066491	0.022099	0.010441
DG(16:0/20:1/0:0)	DG	0.315536	0.27446	0.584002	1.26688	0.325896	0.341448	0.185707	0.036971
DG(16:0/20:3/0:0)	DG	-0.11785	0.567547	3.479046	1.129547	0.427346	0.170898	0.148393	0.045957
DG(18:1/20:0/0:0)	DG	-0.0374	-0.09887	0.028185	1.027809	0.453178	0.371021	0.470814	0.041666
DG(18:2/20:4/0:0)	DG	0.460721	0.585942	0.673665	1.017436	0.046836	0.035854	0.011214	0.029214
(±)12-HETE	Eicosanoid	4.253631	4.206264	3.131	4.833536	0.057189	0.020265	0.08366	0.013177
PGF2α	Eicosanoid	2.559641	1.964423	4.061743	4.120179	0.004386	0.014321	0.003287	0.012599
5-iso PGF2VI	Eicosanoid	0.441651	0.942004	1.046965	3.611075	0.000185	0.00407	0.00081	0.002911
FFA(18:3)	FFA	0.725108	0.713111	1.025713	2.444395	0.000574	0.000413	0.000196	0.000122
FFA(22:4)	FFA	1.052038	1.109519	0.899904	1.148244	0.000766	0.002296	0.000304	0.030227
FFA(22:2)	FFA	0.677078	1.178435	0.971017	1.096585	0.051758	0.056992	0.024603	0.015305
FFA(22:0)	FFA	-1.4544	-2.23349	-2.06996	-1.76132	0.02937	0.008699	0.010351	0.014545
Oleate	Lipids	0.062306	-0.39327	1.544085	-1.27721	0.468427	0.298216	0.179695	0.013633
Hexadecanedioic acid	Lipids_Fatty Acids	1.204368	1.825559	1.045968	1.241864	0.00445	0.022625	0.014219	0.00439
Farnesene	Lipids_Fatty Acids	-2.45454	-2.26485	-2.09316	-2.11914	0.021206	0.099354	0.040713	0.01101
LPA(18:1/0:0)	LPA	1.772428	2.03575	1.915876	1.460178	0.090353	0.063735	0.029694	0.022971
LPC(12:0/0:0)	LPC	1.988682	2.371117	1.801665	1.842264	0.000744	0.003459	5.63E-06	1.13E-05
LPC(O-20:1/0:0)	LPC-O	-1.13589	-1.03422	-1.02353	-1.00529	0.001511	0.001595	0.000814	0.0009
LPE(0:0/20:2)	LPE	3.445042	3.841904	3.703691	3.978356	0.006102	0.003271	0.004961	0.000115
LPE(0:0/16:1)	LPE	-0.07068	0.757932	1.073369	1.106595	0.367639	0.097695	0.012512	0.022061
LPE(0:0/24:6)	LPE	-0.66718	-0.76482	-1.42669	-1.45359	0.02307	0.064546	0.000168	0.000182
(±)12-HEPE [(±)-12-hydroxy-5Z	Oxidized lipid	3.282307	2.116852	2.978332	3.340256	0.012684	0.00107	0.012782	0.008109
(±)12-HETE [(±)12-hydroxy-5Z	Oxidized lipid	4.427983	2.696736	2.907706	2.973186	0.000387	0.035031	0.004601	0.01084
(±)5-HETE [(±)5-hydroxy-6E,8	Oxidized lipid	1.822193	1.731564	2.142326	1.354389	0.053806	0.026535	0.092794	0.03204
PC(18:2/20:4)	PC	-0.78523	-0.74641	-0.95072	-1.00767	0.000684	0.027987	0.00076	5.01E-06
PC(20:2/22:6)	PC	-0.34713	-0.60314	-0.78538	-1.31232	0.109504	0.015342	0.035223	0.000113
PC(18:3/14:1)	PC	-1.00139	-0.50561	-1.45072	-1.34596	0.005548	0.084355	0.000103	0.000236
PC(18:0/20:1)	PC	-0.4436	-1.12383	-1.36652	-1.51313	0.22801	0.058529	0.039548	0.032651
PC(18:0/20:3)	PC	-2.57687	-1.18011	-1.71535	-1.57176	6.98E-05	0.00714	0.000415	0.000609
PC(O-18:2/18:1)	PC-O	-0.9777	-0.95595	-0.96387	-1.13392	0.00296	0.006123	0.003426	0.00221
PC(O-20:2/22:1)	PC-O	-1.47469	-2.09499	-2.08116	-2.99846	0.058423	0.049075	0.035413	0.037923
PE(18:1/16:1)	PE	0.85907	0.896259	1.022551	1.713802	0.029884	0.022072	0.009866	0.001353
PE(16:0/20:3)	PE	0.345407	0.691279	1.102432	1.447521	0.125932	0.030966	0.01512	0.007657
PE(18:3/16:0)	PE	0.481505	1.048007	1.280195	1.403102	0.05584	0.028092	0.00054	0.001459
PE(20:2/16:0)	PE	0.886649	1.029766	0.646767	1.328299	0.00926	0.039204	0.05387	0.025245
PE(18:1/18:1)	PE	0.051414	0.595945	0.706182	1.274643	0.432166	0.130439	0.020859	0.002655
PE(16:1/16:0)	PE	0.646717	1.001911	0.841791	1.254601	0.034365	0.014165	0.024995	0.020742
PE(18:1/18:2)	PE	0.308513	0.834889	0.842207	1.216899	0.118317	0.134253	0.010444	0.002766
PE(18:1/16:0)	PE	0.702429	0.973992	0.941321	1.174923	0.008155	0.005795	0.014999	0.001881
PE(18:2/16:0)	PE	0.856155	1.135298	1.083812	1.155865	0.002932	0.034633	0.011029	0.002504
PE(18:1/20:4)	PE	0.602911	0.785835	0.915018	1.144188	0.00199	0.031528	0.020497	0.005813
PE(22:6/20:1)	PE	1.104173	1.071248	0.733964	1.13255	0.009958	0.00137	0.052794	0.005557
PE(18:2/14:0)	PE	0.22172	0.855868	1.058296	1.1133	0.314543	0.116606	0.003648	0.003145
PE(14:0/22:6)	PE	0.684661	1.148661	1.379301	1.071759	0.055355	0.05452	0.007193	0.00542
PE(18:1/18:0)	PE	0.247405	0.584922	0.709438	1.052673	0.192325	0.12131	0.035315	0.014822
PE(16:1/18:0)	PE	0.340382	0.808883	0.727173	1.021532	0.07113	0.010672	0.005481	0.002107
PE(20:4/22:2)	PE	0.036104	-0.55366	-1.12848	-1.40203	0.461089	0.153713	0.001719	0.000171
PE(P-18:2/16:0)	PE-P	-0.65967	-0.82465	-0.86965	-1.0651	0.048543	0.074287	0.005285	4.47E-05
PE(P-18:2/20:3)	PE-P	-0.79807	-1.1557	-1.2334	-1.11779	0.001253	0.000122	3.73E-06	1.24E-05
PE(P-20:2/20:2)	PE-P	-1.56728	-1.43213	-1.64054	-1.27486	7.03E-06	3.69E-05	5.37E-06	3.28E-05
PE(P-18:2/18:2)	PE-P	-0.52204	-0.80443	-1.12382	-1.40226	0.052181	0.017829	0.000576	0.000172
PE(P-18:2/20:2)	PE-P	-1.12596	-1.38181	-1.62322	-1.46111	0.000141	2E-05	6.23E-07	1.71E-06
PE(P-18:2/18:1)	PE-P	-1.34364	-1.71902	-1.88436	-1.91779	0.00019	1.29E-05	6.29E-06	6.41E-06
PE(P-18:2/20:1)	PE-P	-1.3963	-1.54926	-1.80592	-2.00009	0.080513	0.054312	0.107416	0.039186
PE(P-18:2/18:3)	PE-P	-1.59694	-0.87394	-1.16568	-2.07055	0.034617	0.032079	0.072561	0.022068
PI(18:2/18:0)	PI	1.24128	1.100703	0.976307	1.097714	0.010891	0.067275	0.053573	0.030691
PS(18:1/22:6)	PS	1.929859	1.939216	1.816299	1.643889	0.000168	0.001636	0.008221	0.00035
TG(14:0/22:1/22:3)	TG	2.530847	3.163348	3.558783	4.170396	1.71E-05	1.86E-05	1.97E-05	1.88E-05
TG(18:2/18:3/20:4)	TG	1.907355	2.187941	2.712237	2.674074	0.029254	0.036686	0.064876	0.044103
TG(18:3/18:3/18:3)	TG	-1.35806	-0.1598	0.454331	2.591791	0.030745	0.008457	0.010362	0.009289
TG(18:1/18:1/20:0)	TG	-0.67098	0.062852	0.606658	2.179717	0.013116	0.00902	0.007992	0.00748
TG(16:0/18:0/22:3)	TG	1.474583	1.821977	1.586085	2.106836	0.123512	0.469439	0.002025	0.001996
TG(14:0/22:3/22:4)	TG	1.224878	1.453811	1.261318	1.878186	0.015747	0.011317	0.003613	0.006113
TG(14:0/20:2/22:2)	TG	0.828815	1.400443	1.212017	1.86619	0.014444	0.005438	0.008918	0.003713
TG(18:1/18:3/20:0)	TG	0.217134	0.744181	0.861473	1.664225	0.261735	0.033303	0.024577	0.01095
TG(14:0/22:4/22:4)	TG	2.284213	2.586025	1.604119	1.476575	0.002087	0.047008	0.012708	0.034105
TG(18:2/18:2/20:0)	TG	0.136132	0.657789	0.66104	1.35712	0.323551	0.03156	0.043491	0.01094
TG(16:1/20:1/20:2)	TG	-0.12746	0.431547	0.363936	1.317693	0.328337	0.083451	0.153521	0.030472
TG(14:0/20:1/22:2)	TG	-0.01997	0.435417	0.498753	1.179537	0.473213	0.087141	0.078368	0.025326
TG(14:0/20:5/22:4)	TG	0.862815	1.448211	1.096723	1.171199	0.01581	0.052076	0.005474	0.026708
TG(14:0/20:5/22:3)	TG	0.958314	1.25658	1.289513	1.164696	0.007246	0.022542	0.003835	0.00589
TG(14:0/18:3/22:1)	TG	0.143305	0.530674	0.574017	1.14321	0.296111	0.071882	0.065143	0.039756
TG(14:1/14:1/22:3)	TG	0.411214	0.858473	0.458976	1.110463	0.058527	0.078951	0.062302	0.043672
TG(14:0/20:1/20:1)	TG	0.509187	0.821977	0.776724	1.10684	0.051154	0.004146	0.01739	0.008423
TG(14:0/20:2/22:4)	TG	-0.01118	0.553877	0.307815	1.106744	0.488277	0.149325	0.185823	0.013816
TG(18:1/18:3/20:1)	TG	-0.50991	0.373252	0.070203	1.096099	0.102354	0.162646	0.426741	0.021715
TG(14:0/20:3/22:1)	TG	0.084783	0.4021	1.001136	1.078581	0.421262	0.126518	0.068758	0.003347
TG(18:1/18:3/20:4)	TG	0.852752	1.108224	1.292052	1.077181	0.017804	0.017154	0.005894	0.009172
TG(18:0/18:1/18:2)	TG	0.384664	0.433441	0.528006	1.040391	0.083429	0.008009	0.04538	0.0036
TG(16:0/20:4/22:5)	TG	1.020815	0.976493	1.772852	1.035576	0.00601	0.017401	0.021907	0.048099
TG(14:0/20:3/20:5)	TG	0.554584	1.000365	0.992563	1.035273	0.115594	0.081054	0.038692	0.041673
TG(18:0/18:3/20:2)	TG	-0.07914	0.430927	0.267478	1.001518	0.411076	0.128127	0.222412	0.014944
TG(14:0/20:0/20:0)	TG	-2.94121	-4.26743	-3.90332	-3.53402	0.021052	0.023798	0.026928	0.026418

Table S9. Lipidomic data of S vs H and M vs H

		Log_2 FC				*P* value			
Compounds	Class	ST1/H	ST2/H	MT1/H	MT2/H	ST1/H-P	ST2/H-P	MT1/H-P	MT2/H-P
Glycocholic Acid	Bile Acids	-1.56256631	-1.734053726	-1.9023288	-2.27865103	0.02306349	0.015077963	0.0122502	0.008120827
Cer(d18:1/18:1)	Cer	3.103373474	2.694176315	2.087149306	2.386808302	0.035759384	0.000440324	0.000512193	0.012090853
Cer(d18:0/18:0)	Cer	1.806648121	2.023396674	2.062599441	2.280526728	0.016516581	0.015809763	0.017251447	0.00675199
DG(16:0/20:2/0:0)	DG	3.419566256	4.760460977	3.790298648	4.230188035	0.012879856	0.022808216	0.010695387	0.014146693
DG(14:1/22:3/0:0)	DG	1.946986599	2.52513302	2.184108717	2.562694047	0.011953867	0.040682557	0.001654452	0.055821581
DG(16:0/16:1/0:0)	DG	1.343366759	2.446915514	2.235581794	2.947646712	0.025046109	0.040006045	0.001941206	0.000638302
DG(16:1/18:3/0:0)	DG	1.615029147	1.258379545	1.712432931	1.621531685	0.001638189	0.017733488	3.79113E-05	4.53497E-05
DG(16:1/20:2/0:0)	DG	1.158272128	2.067739658	1.716402514	1.976972407	0.045185513	0.020005295	0.001901897	0.001195212
FFA(22:0)	FFA	-1.68042683	-1.715484992	-1.52646973	-1.97087192	0.017237641	0.01695126	0.020915218	0.011453033
LPC(12:0/0:0)	LPC	1.592738534	1.677657267	1.879575129	2.131799559	0.000213342	0.000792147	2.63225E-07	1.0296E-07
(±)12-HEPE [(±)-12-hydrc	Oxidized lipid	1.203063199	1.994467481	2.472382374	3.143034687	0.01085773	0.022254719	0.000927184	0.004009076
PC(18:0/20:3)	PC	-1.93876945	-1.093608196	-1.22370115	-0.81168844	0.000176746	0.003882864	0.002374377	0.020975714
PC(O-20:2/22:1)	PC-O	-1.24441276	-2.774862923	-2.57911573	-1.34196972	0.029745143	0.027803613	0.02724922	0.027952109
PE(18:2/20:4)	PE	1.194094437	0.937574948	1.057427307	0.734281086	0.002428119	0.008602052	0.001564624	0.030090036
PE(P-18:0/18:0)	PE-P	-1.33073606	-0.612572106	-1.17321132	-0.35203395	7.82174E-06	0.015574562	1.12867E-05	0.024522692
PI(18:2/18:0)	PI	1.166854807	1.717360487	1.600095702	1.643987518	0.000275676	0.000773877	0.006566721	0.00147547
PS(18:1/22:6)	PS	1.91441964	1.740121496	1.830156627	1.866477265	0.001905388	0.000790976	5.03158E-06	6.39596E-06
TG(14:0/22:1/22:3)	TG	2.45514207	3.332584857	2.912408929	3.142038268	1.99341E-05	2.08032E-05	1.94126E-05	2.25595E-05
TG(18:2/18:3/20:4)	TG	1.956422308	2.626290364	2.971456773	2.741472617	0.012330324	0.010373693	0.000184251	3.41608E-06
TG(14:0/22:3/22:4)	TG	1.110069554	1.001875522	1.249508459	1.388617688	0.027841387	0.065652631	0.001623118	0.008041958
TG(14:0/20:2/22:2)	TG	1.104910867	1.287741589	1.210856405	1.593205222	0.028105753	0.024176167	0.001506904	0.002423129
TG(14:0/20:0/20:0)	TG	-3.78438956	-0.839636612	-2.12205027	-0.29733705	0.02549273	0.032673181	0.028730109	0.035735915

Table S10. KEGG enrichment analysis of DEIs shared by F vs H, S vs H and M vs H

#KEGG	n 16	KEGG N	524			
#Pathway	ko ID	Unique con	compound	Uni all	compound	all
Metabolic p	ko01100	14	418	16	524	LIPID-N-0 C01194+C00641+C02737+C00157+C00422+C00195+C00641+C00422+C00422+C00422+C00641+C00641+C00641+C00422
Adipocytok	ko04920	2	46	16	524	LIPID-N-0 C00162+C00195
Insulin resi	ko04931	7	237	16	524	LIPID-P-1 C00422+C00422+C00422+C00195+C00422+C00422+C00162
Leishmania	ko05140	2	17	16	524	LIPID-P-0(C00195+C02737
Glycerolipi	ko00561	11	287	16	524	LIPID-P-0 C00641+C00641+C00422+C00641+C00641+C00422+C00422+C00422+C00422+C00162+C00641
Inositol ph	ko00562	6	56	16	524	LIPID-P-0 C00641+C00641+C00641+C00641+C01194+C00641
Glycerophc	ko00564	9	217	16	524	LIPID-P-0 C00641+C00641+C01194+C00641+C00641+C02737+C00641+C00157+C04230
Phosphatid	ko04070	6	59	16	524	LIPID-P-0 C00641+C00641+C00641+C01194+C00641+C00641
Long-term	ko04730	5	55	16	524	LIPID-P-0 C00641+C00641+C00641+C00641+C00641
Thermogen	ko04714	6	227	16	524	LIPID-P-1(C00422+C00162+C00422+C00422+C00422+C00422
Regulation	ko04923	6	227	16	524	LIPID-P-1(C00422+C00422+C00422+C00162+C00422+C00422
Fat digestic	ko04975	6	234	16	524	LIPID-P-0' C00422+C00422+C00422+C00162+C00422+C00422
Vitamin di	ko04977	6	231	16	524	LIPID-P-1 C00422+C00422+C00162+C00422+C00422+C00422
Cholesterol	ko04979	6	229	16	524	LIPID-P-0' C00422+C00422+C00422+C00422+C00422+C00162
Choline me	ko05231	3	123	16	524	LIPID-P-0' C04230+C00157+C00162

Table S11. KEGG enrichment analysis of DEIs unique to F vs H

#KEGG : 58 KEGG N: 524

#Pathway	ko ID	Unique co	commonl	Uni	all	commonl	all
Glycerolip	ko00561	32	287	58	524	LIPID-P-(	C00422+C00422+C00423+C00641+C00422+C00681+C00422+C00422+C00422+C00641+C00162+C00162+C00422+C00641+C00422+C00422+C00641+C00422+C00422+C00641+C00422+C00641+C00422+C00162+C00422+C00422+C00422+C00422+C00641+C00422
Inositol-ol	ko00562	7	56	58	524	LIPID-P-(	C00641+C00641+C00641+C00641+C00641+C00641+C00641
Glycerol	ko00564	31	217	58	524	LIPID-P-(	C00350+C00438+C00350+C00641+C00641+C00641+C00350+C00641+C00350+C00157+C00350+C00350+C00438+C00350+C00350+C00350+C00681+C00350+C00350+C00641+C00157+C00438+C00157+C00350+C00350+C00350+C00350+C00641+C00157+C00350+C00641
Metabolic	ko01100	51	418	58	524	LIPID-P-(	C00350+C00422+C00422+C00422+C00422+C00422+C00641+C00422+C00639+C136115+C00350+C00350+C00422+C00422+C00350+C00422+C00422+C00157+C00641+C00422+C00350+C00350+C00350+C00350+C00641+C00350+C00422+C00350+C00641+C00422+C00641+C00350+C00641+C00422+C00641+C00422+C00422+C00157+C00422+C00422+C00350+C00350+C00350+C00681+C00422+C00422+C00422+C00157+C00422+C00422+C00157+C
Phosphati	ko04070	7	59	58	524	LIPID-P-(	C00641+C00641+C00641+C00641+C00641+C00641+C00641
Longevity	ko04730	7	55	58	524	LIPID-P-(	C00641+C00641+C00641+C00641+C00641+C00641+C00641
Arachidon	ko00590	5	59	58	524	LIPID-N-	C00359+C00157+C00157+C00157+C00157
Sphingolip	ko00600	2	7	58	524	LIPID-N-	C00639+C00639
Neurotroph	ko04080	2	5	58	524	LIPID-P-(	C00681+C00639
Fatty acid	ko00062	3	34	58	524	LIPID-N-	C00162+C00162+C00162
Fatty acid	ko00071	3	35	58	524	LIPID-N-	C00162+C00162+C00162
AMPK sig	ko04152	3	33	58	524	LIPID-N-	C00162+C00162+C00162
Thermogen	ko04714	24	227	58	524	LIPID-P-	C00422+C00422+C00422+C00422+C00422+C00422+C00422+C00422+C00162+C00422+C00422+C00422+C00422+C00422+C00422+C00422+C00422+C00162+C00422+C00422+C00422+C00422+C00162
Insulin se	ko04911	3	33	58	524	LIPID-N-	C00162+C00162+C00162
Adipocyte	ko04920	3	46	58	524	LIPID-N-	C00162+C00162+C00162
Regulatio	ko04923	24	227	58	524	LIPID-N-	C00162+C00162+C00422+C00422+C00422+C00422+C00422+C00422+C00422+C00422+C00422+C00422+C00422+C00422+C00422+C00422+C00162+C00422+C00422+C00422+C00422+C00422+C00422
Toxo. E.d	ko04930	3	33	58	524	LIPID-N-	C00162+C00162+C00162
Insulin re	ko04931	24	237	58	524	LIPID-P-	C00422+C00422+C00422+C00422+C00422+C00422+C00422+C00422+C00162+C00422+C00422+C00422+C00422+C00422+C00422+C00422+C00422+C00422+C00422+C00422+C00422+C00162+C00162
Non-alcoh	ko04932	3	33	58	524	LIPID-N-	C00162+C00162+C00162
Fat digest	ko04975	25	234	58	524	LIPID-P-	C00422+C00422+C00422+C00422+C00422+C00422+C00422+C00422+C00422+C00422+C00162+C00422+C00162+C00422+C00422+C00162+C00422+C00422+C00681+C00422+C00422+C00422+C00422+C00422+C00422
Vitamin d	ko04977	25	231	58	524	LIPID-P-	C00422+C00422+C00422+C00422+C00422+C00422+C00422+C00162+C00422+C00422+C00422+C00422+C00422+C00422+C00422+C00422+C00422+C00422+C00681+C00422+C00422+C00422+C00162+C00162+C00422+C00422+C00422+C00422
Cholesterol	ko04979	24	229	58	524	LIPID-P-	C00422+C00422+C00422+C00422+C00422+C00422+C00422+C00162+C00422+C00422+C00422+C00422+C00162+C00422+C00422+C00422+C00422+C00422+C00422+C00422+C00422+C00422+C00422+C00422+C00422
Choline m	ko05231	7	123	58	524	LIPID-N-	C00162+C00157+C00162+C00162+C00157+C00157+C00157
Linoleic a	ko00591	4	63	58	524	LIPID-P-(	C00157+C00157+C00157+C00157
alpha-Lin	ko00592	4	57	58	524	LIPID-P-(	C00157+C00157+C00157+C00157
Retinoym	ko04723	20	99	58	524	LIPID-N-	C00350+C00350+C00157+C00157+C00350+C00350+C00350+C00157+C00157+C00350+C00350+C00350+C00350+C00350+C00350+C00350+C00350+C00350+C00350
Glycosylp	ko00563	16	46	58	524	LIPID-N-	C00350+C00350+C00350+C00350+C00350+C00350+C00350+C00350+C00350+C00350+C00350+C00350+C00350+C00350+C00350+C00350
Autophar	ko04136	16	46	58	524	LIPID-N-	C00350+C00350+C00350+C00350+C00350+C00350+C00350+C00350+C00350+C00350+C00350+C00350+C00350+C00350+C00350+C00350
Autophag	ko04140	16	46	58	524	LIPID-N-	C00350+C00350+C00350+C00350+C00350+C00350+C00350+C00350+C00350+C00350+C00350+C00350+C00350+C00350+C00350+C00350
Pathogeni	ko05130	16	44	58	524	LIPID-N-	C00350+C00350+C00350+C00350+C00350+C00350+C00350+C00350+C00350+C00350+C00350+C00350+C00350+C00350+C00350+C00350
Kaposi sa	ko05167	16	44	58	524	LIPID-P-(	C00350+C00350+C00350+C00350+C00350+C00350+C00350+C00350+C00350+C00350+C00350+C00350+C00350+C00350+C00350+C00350

Table S12. Normalized expression levels of potential biomarkers

Compounds	Class	F1T4	F2T4	F3T4	F4T4	F5T4	F6T4	F7T4	F8T4	F9T4	S1T1	S2T1	S3T1	S4T1	S5T1	S6T1	S7T1	S8T1	S9T1	S10T1	S11T1	M1T1	M2T1	M3T1	M4T1	M5T1	M6T1	M7T1	M8T1	M9T1	M10T1	M11T1	M12T1	M13T1	M14T1	H1	H2	H3	H4	H5	H6	H7	H8	H9	H10
L-Malic Acid	Amino Acid metabolomics	45176	26322	26412	41652	26018	76817	44656	15549	14220	53091	46098	51620	22305	25626	35500	23009	28114	17275	25686	104128	40712	15970	23186	52440	20737	18179	40892	46765	41558	112180	41061	48789	278200	18094	10346800	10705500	2856858	4264400	2154408	4325260	3917770	5108638	1474000	2684000	2684000
Carbamoyl phosphate	Organic Acid And Its Derivatives	59403	9952	56363	16807	40263	10722	41912	152420	58902	55099	56038	111290	20204	81407	19372	26351	150440	143670	141739	16348	25265	49481	60299	115510	86155	162990	121170	92955	93483	110180	185910	145270	72272	98112	12537000	10046600	296350	9199920	8164400	5577790	6376560	8152836	344130	2580050
D-Tyloloso 5-phosphate	Carbohydrate metabolomics	171080	72049	206800	48742	199830	79214	108230	234050	455140	152000	213729	199040	185700	261010	132600	261910	207660	352130	324540	226330	135260	166060	224020	221750	279580	256750	234050	293070	215820	115170	308200	385380	289830	193410	511860	666320	693750	849010	815030	638000	531990	367610	498610	675490
Guanosine Monophosphate	Nucleotide metabolomics	51051	49547	16586	6964.3	6729	6868.6	5359.8	4826	9827.8	11746	17387	36354	63113.8	23073	8821.1	6596.5	25740	67617.4	16594	12378	48518	16102	8525.1	26282	16077	25167	40546	13713	35162	48338	46529	7669.3	37132	41968	27895	75990	45363	43012	32968	23892	21975	69866	46231	24129
Dihydroorotate	Nucleotide metabolomics	16170	13595	40482	13987	11085	55976	25089	60296	15161	28254	26867	34815	18760	30813	11779	21987	93501.9	51484	41913	22199	28129	8087	5101.4	31517	36729	40448	34815	41796	23643	44913	18424	65827	44179	47542	50240	106380	164110	200290	92012	155010	108580	198750	63011	20094
FFA(22:0)	FFA	231930	72724	64112	224330	115360	183530	67835	264130	252650	87084	106140	79672	73800	84010	74028	74832	71497	295170	326820	434960	77366	57674	68931	82116	112480	88856	74417	113070	186910	263590	510740	355990	251140	535810	1318890	155150	251740	410430	604060	782860	1445600	1276300	62322	236630
CE(20:1)	CE	26615	15208	41461	10361	11757	28876	457.99	457.56	5701.6	2232.4	10721.6	1426.8	2444.1	4442	1591.2	2666.1	3832.3	273.82	328.41	335.91	1266.8	2094.7	676.42	1786.4	4485.8	2730.4	1518.6	2160.1	2765.4	585.43	381.82	196.25	104.39	445.47	16078	20145	3444.3	19263	23204	22188	641.91	341.91	468.01	272.3
LPC(O-20:1/0:0)	LPC-O	46253	55294	98328	48869	86851	173070	99156	104900	154160	40864	106770	77475	50666	123370	17146	124790	107280	147680	129820	91985	118170	74701	122960	131590	117950	89784	78947	143110	162370	133230	227500	178310	152740	275360	263210	294540	229030	116920	87362	164160	202240	267640	132730	219900
PC(18:0/20:1)	PC	25464	15915	43066	13901	64679	1460.7	72155	2130.1	70690	12674	23946	24659	32582	30773	16066	88624	18765	12945	7467.2	3682.3	60341	26236	24084	81991	30540	43510	25218	61672	69888	2840.3	8406.4	3098.2	1458.4	162520	123600	108400	82138	3884	84363	132210	89416	175808	96410	125910
PE(P-20:2/20:2)	PE-P	56996	26402	100890	160390	49123	95423	109900	104430	65404	31175	67571	59775	113610	142840	9212.3	251540	121970	54607	68910	57631	97846	30996	99488	107200	190040	133110	51892	117110	110040	127150	118900	163630	95682	130620	141110	259700	147800	158260	244080	238040	276320	140758	185330	285300
Glycerol 3-sebacate	Lipids Fatty Acids	171900	115500	208950	90410	140960	191470	106170	125600	727750	98015	193520	160640	204280	186740	108040	204040	110580	63720	417670	191240	80553	148700	157170	111110	150170	191760	158140	215210	144500	104590	515200	98096	444470	420710	4569700	5710700	3843200	576100	5291100	6621000	2019600	2627000	4054000	946440
Hydroxycitrulline Acid	Bile Acids	11259	94893	8.1249	11.655	10.079	39858	4417.6	7813.9	576.95	11.008	10.381	10.286	9.4448	9.6626	11912	5244.2	8.7601	17911	72259	3931.6	13.936	8.8008	7.8142	30224	32729	7.8397	70758	6471.1	8946.6	11228	15703	8726.4	8163.1	5029.1	26278	11153	176360	43926	16658	42218	48699	118690	28941	208320
2-Methylbutyroylcarnitine	Acylcarnitines	1.8E+07	1.4E+07	1.8E+07	1.8E+07	1.8E+07	1.8E+07	1.8E+07	1.8E+07	1.8E+07	1.8E+07	1.8E+07	1.8E+07	1.8E+07	1.8E+07	1.8E+07	1.8E+07	1.8E+07	1.8E+07	1.8E+07	1.8E+07	1.8E+07	1.8E+07	1.8E+07	1.8E+07	1.8E+07	1.8E+07	1.8E+07	1.8E+07	1.8E+07	1.8E+07	1.8E+07	1.8E+07	1.8E+07	1.8E+07	1.8E+07	1.8E+07	1.8E+07	1.8E+07	1.8E+07	1.8E+07	1.8E+07	1.8E+07	1.8E+07	1.8E+07
LPE(0:0/20:2)	LPE	14953	3165.2	2988	5320.8	12296	10260	10012	9067	20871	2246.1	10962	24613	63775.8	13412	986.74	8351.8	15014	21381	11606	14324	10348	5225.4	17385	16658	96394	60363	71512	8755.9	14813	45670	16427	12634	17962	23091	796.45	462.35	929.53	422.49	287.54	270.96	134.68	1926.3	1718.9	894.56
DG(16:0/20:2/0:0)	DG	13831	4797.9	33501.6	19104	14762	5377.8	12634	6520	17112	457.82	2656.8	2226.5	16336	5425.4	705.99	8292	6554.2	7452.8	9281.4	13312	4887.4	2511.5	3851.6	16549	4834.8	10402	31368.8	7039.1	9357.1	5766.1	16583	13010	4910.6	13857	582.67	918.01	933.59	191.97	688.71	802.86	586.31	556.65	556.42	609.95
DG(14:0/22:5/0:0)	DG	4448.1	5901.1	2420.9	2587.6	4595.4	5551.6	10522	18222	9922	282.90	2663.3	2765.2	6035.3	3068.7	726.58	3032.9	6907	2405.4	4901	13908	5208.1	16969	39017	10497	2987.7	5311.8	2879.7	7595.9	9104.2	6157.7	5928.5	18484	4876.5	2112.6	235.21	276.34	564.43	594.55	2960.3	1860	2114.5	488.54	241.42	780.03
LPC(12:0/0:0)	LPC	513930	524510	676430	399410	574970	832630	898030	787060	953480	328760	552470	269900	525450	557450	228738	463020	628140	877880	951020	941330	526140	589730	592630	479730	634430	673860	481040	487780	626580	1068400	1010300	1020500	743190	1008200	194820	170180	265860	217720	172050	87845	307780	71856	149020	278320
PS(18:1/22:6)	PS	15191	15648	10171	63481	7973.6	10260	17998	23123	13589	4947.7	16964	4057.1	11884	17085	5121.8	13518	21818	34485	11883	32292	15251	8876	12614	6743.1	13898	13159	10757	11453	14852	26810	15111	19429	21062	19405	7838.5	11816	1955	1875.8	3167.6	1505.5	4838.4	597.68	14234	5218.5
TG(14:0/22:1/22:3)	TG	14734	5232.4	36802	2257.8	2258	6788.5	4805.4	190.24	6310.9	214.9	801.77	107.5	4090.8	1919.4	413.63	718.9	1776.5	224.94	1736	3981.4	817.43	276.38	3416.9	1807	1248.5	1159.6	695.68	875.73	563.48	358.8	4896.5	4409.4	1399.3	4898.4	266.74	203.59	79.879	145.2	63.609	123.88	80.145	1132.8	69.136	485.16
TG(18:2/18:3/20:4)	TG	24164	9620.8	17332	143380	93903	55883	18734	47921	32765	12241	37259	14758	36514	54988	5257.8	20721	21385	64519	24459	45677	36998	14054	35862	125380	30975	31651	36435	10867[illegible]	98605	49596	117940	63639	44740	68664	17263	2378.6	2992.1	3842.7	5575.7	2001	6228.3	23197	8204.7	5527.6

Table S13. Clinical characteristics of COVID-19 patients in this study

	Fatal (n=9)				Severe (n=11)		Mild (n=14)	
	F1	**F2**	**F3**	**F4**	**S1**	**S2**	**M1**	**M2**
Characteristic								
ALT (normal range 9-50 U/L)	46(22-66)	31(22-49)	39(27-59)	40(29-109)	39(24-56.5)	47(32.5-78.5)	29(13.8-37.5)	33(25.5-65)
AST (normal range 15-40 U/L)	38(34-74)	44(25-53)	32(27-42)	56(41-228)	29(24-43)	33(21.5-36.5)	26.5(20.3-30.3)	22.5(14.3-27.8)
Total bilirubin (normal range 0-21 μmol/L)	15(12-21.2)	25.6(12.2-35.1)	17.5(16.1-23.5)	18.3(16.2-19.7)	10.5(10-13.6)	10.1(7.55-13.1)	13.3(11-16.8)	9.3(7.4-11.4)
Patients with pre-existing liver conditions	1 (11.1%)				0 (0%)		2 (14.3%)	

Data are median (IQR)